



Fabrication of bisferrocenyl derivative grafted HTPB with high iron content and its application in dopamine detection

Alireza Aghaiepour, Shabnam Rahimpour, Elmira Payami, Reza Mohammadi, Reza Teimuri-Mofrad*

Department of Organic and Biochemistry, Faculty of Chemistry, University of Tabriz, 51664 Tabriz, Iran

ARTICLE INFO

Article history:

Received 27 December 2020

Revised 4 March 2021

Accepted 20 March 2021

Available online 22 March 2021

Keywords:

Bis-nuclear ferrocene

Alkylferrocene

Hydrosilylation reaction

Modified polymer

Dopamine detection

ABSTRACT

In this work, we employed an efficient strategy to increase the graft percentage of ferrocene in hydroxyl terminated polybutadiene (HTPB) polymer framework. For this purpose, we use 5-chloro-2-pentanone to attach the two alkylferrocene derivatives to each other. In order to incorporate the obtained bis-alkylferrocene derivatives to the polymer backbone, the chlorine atom at the end of the coupling agent alkyl chain was converted to a silane group using the Grignard reaction. Finally, hydrosilylation reaction of as-synthesized silane derivatives and HTPB in the presence of Speier's catalyst (H_2PtCl_6) resulted in novel bis-ferrocene modified HTPBs with a variety of iron contents. The iron percentage, viscosity, and glass transition temperature of the novel bis-ferrocene modified HTPBs as essential parameters of polymer characterization were investigated. Obtained polymers are electro-active due to the presence of ferrocenyl groups. Additionally, unlike the virgin polymer (HTPB) they show optical properties. The final polymer was immobilized onto the bare glassy carbon electrode (GCE) surface using the cross-linking effect of terephthaldehyde (TFA) and fresh egg white (FEW). Electrochemical impedance spectroscopy (EIS) confirmed the successful immobilization of the polymer. The ability of the fabricated electrode to mediate dopamine (DA) oxidation was evaluated, and the results show the acceptable detection limits as well as linear ranges for the determination of dopamine using GC/BEFCHTPB/(TFA+FEW).

© 2021 Elsevier B.V. All rights reserved.

1. Introduction

Dopamine (DA) is a vital substance in the life of Mammals, which roles as a catecholamine neurotransmitter in the central nervous system (CNS) also a hormone in the blood [1–3]. Recently, abnormal DA concentrations have been shown to cause neurological disorders such as cases Alzheimer's disease, Schizophrenia, Parkinson's disease, pheochromocytoma, and attention deficit hyperactivity disorder [4–6]. Dopamine is an essential drug used to treat heart failure diseases, especially for premature infants [7]. In recent years, much energy has been devoted to the detection of dopamine. Conventional methods utilized for the detection of dopamine are performed using analytical techniques such as chemiluminescence [8], capillary electrophoresis [9], liquid chromatography [10], mass spectrometry [11], optical or electrochemical detection [12]. However, the most economical, fast and affordable method is the use of electrochemical sensing tech-

niques to detect electroactive neurotransmitters, including uric acid, dopamine, ascorbic acid and etc [13].

Recently, direct electrochemical methods (redox on the modified electrode surface) have received much attention for dopamine detection due to their simplicity, high-speed response, and high sensitivity, as well as their wide linear relationship [14–16]. On the other hand, other electroactive substances, such as ascorbic acid (AA) interfere with the detection of dopamine [17]. Therefore, to solve this problem, simple electrodes (glassy carbon [18], graphene oxide [19], carbon nano-tubes (CNTs) [20], Au electrode and etc [21],) have been modified and examined via cellulose microfibril (CMF) [22,23], chitosan [6], cyclic oligosaccharides such as β -cyclodextrin [3], CuS nanoplates [24], inorganic dye [25], copper (II) complex [26], and organometallic compounds [27,28]. Some of the recent development of advanced dopamine sensors were summarized in Table 1.

There is more interest in recent decades on ferrocene derivatives specially alkylferrocenes. The use of ferrocenyl compounds in electrochemical devices [33], optical systems [34], asymmetric organometallic catalysis [35], chiral cancer drugs and other fields [36], is because of their unique planar chirality properties, thermal, optical, and redox behaviors. In addition, alkylferrocene with

* Corresponding author.

E-mail address: teymouri@tabrizu.ac.ir (R. Teimuri-Mofrad).

Table 1

Some of the recent advanced modified electrodes for dopamine sensors.

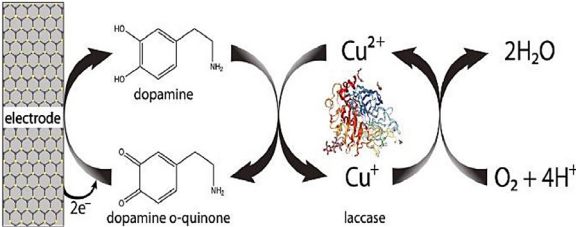
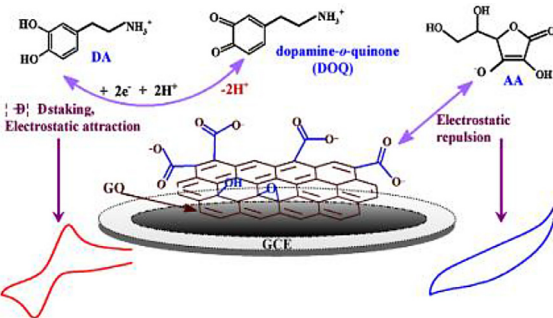
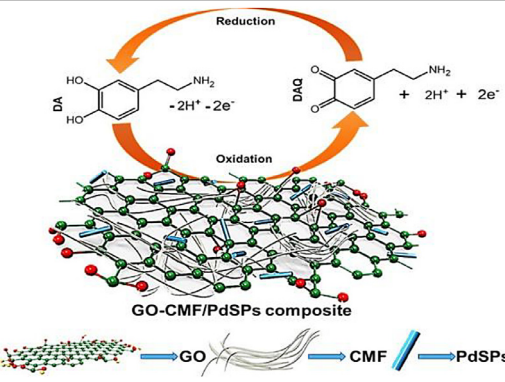
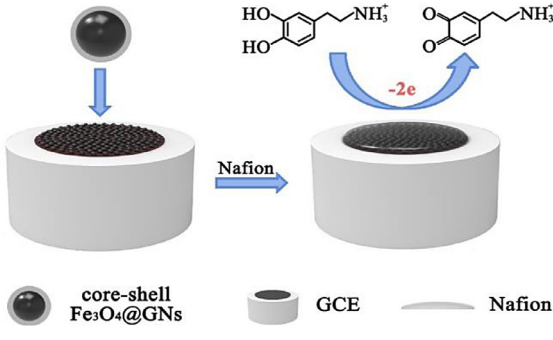
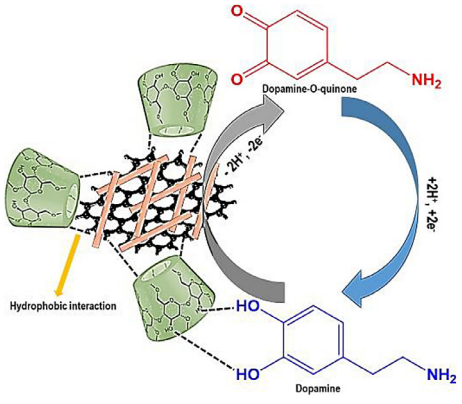
Entry	Prepared electrode	Some of the advantages	Ref
1		determination of dopamine in citric acid/KOH buffer sensitivity: 340.3 nA/ μ M LOD: 10 nM	[29]
2		Selective detection dopamine in the presence of ascorbic acid and uric acid (UA). Linear response ranges: 1 μ M to 100 μ M LOD: 0.1 μ M	[30]
3		Selective detection of DA in the presence of some electroactive compounds. Linear response ranges: up to 196.3 μ M LOD: nano molar	[22]
4		determination of dopamine in 0.1 M PBS (pH 7.0) Selective determination of DA in the presence of AA and UA. Linear response ranges: 0.02 μ M to 130 μ M LOD: 0.007 μ M	[31]

Table 1
(Continued).

Entry	Prepared electrode	Some of the advantages	Ref
5		Selectivity for DA in the presence of 50 folds additions of potentially active interfering compounds. Linear response ranges: up to 150.76 μM LOD: 4 nM 99.2% Recovery of DA in the rat brain	[32]

the capability to form an aqueous micellar pseudo phase can be used as a biosensor. For example, the electrochemical properties of ferrocene in coupling with some biomolecules such as glucose oxidase can be used as a biosensor for the determination of the glucose in aqueous solution [37]. At first, alkylferrocenes were synthesized directly from alkyl cyclopentadienes [38], but now many routes are used for the synthesis of corresponding alkylferrocenes from ferrocene as a primary substance. Generally, alkylferrocene derivatives are prepared via a two-step route include Friedel-Crafts acylation of ferrocene followed by the reduction of the acylated ferrocene [39].

Nowadays, grafting of ferrocene and its derivatives onto polymers backbone has attracted a lot of attention because it offers unique properties to the obtained modified polymer. Redox-switchable behavior for electrochemical-induced drug delivery systems in aqueous medium [40], role playing electroactive groups on supercapacitor composites [41], Hyperbranched Polymer films containing organometallic groups [42], burning rate accelerator catalyst for airbags and other safety devices [43,44], as well as, ferrocene grafted hydroxyl terminated polybutadiene (HTPB) as a burning rate accelerator are the examples of such applications [45].

Although, HTPB is not a very famous polymer, it has ideal physical properties include high loading capacity, storage capacity, low viscosity, ability to decrease the vulnerability of explosives, high mechanical-thermal stability and sub-ambient glass transition temperature [46].

Herein, to continue our previous attempts on ferrocene-based compounds and their successful grafting on some polymers [41,47–49], we describe the synthesis of bis-alkylferrocenyl silane compounds via condensation reaction of as-prepared alkylferrocenes by appropriate ketone compound. Silylation of obtained bis-alkylferrocene allows the ferrocenyl group to be introduced to HTPB backbone via hydrosilylation reaction. Optical and electrochemical properties of the novel modified polymer and other important parameters such as iron percentage, viscosity and glass transition temperature were investigated. In continue, the modified electrode was prepared via [4,4-Bis(ethylferrocenyl)pentyl]dimethylsilane grafted HTPB containing 15.98% of Fe (4a'', BEFCHTPB) as the representative of final ferrocenyl polymers, terephthalaldehyde (TFA), and fresh egg white (FEW). The success of the electrode modification was confirmed by electrochemical impedance spectroscopy (EIS). The prepared elec-

trode showed an excellent electrocatalytic effect on the oxidation of dopamine to quinone dopamine. The morphology studies, cyclic voltammetry (CV), differential pulse voltammetry (DPV), effect of pH, selective determination of DA in the presence of AA and electrochemical properties of DA on the GC/BEFCHTPB/(TFA/FEW) electrode were also investigated.

2. Experimental

2.1. Materials and instrumentation

All commercial compounds were purchased from Sigma-Aldrich and used without any purification. ^1H -NMR spectra were obtained with Bruker FT-400 spectrometer in CDCl_3 , the FT-IR spectra were reported with Bruker-Tensor 270 spectrometer on KBr disk. The mass spectra were obtained with 70 eV by Agilent (5975C VL) instrument, the most important peaks were reported in m/z units with M^+ as the molecular ion. The Elemental analyses were carried out with an Elementor Vario EL III instrument. The Analytikjane (nova 400) atomic absorption spectrophotometer was used for iron analysis. The Brook field RVT viscometer was used for viscosity measurement. The SPECORD 250 analytik jena UV/Vis spectrophotometer was used for recording the electronic absorption spectra. The Field Emission Scanning Electron Microscopy FE-SEM (MIRA3 TESCAN) was used for surface morphology studies. Cyclic voltammetry measurements were performed on synthesized polymers in dichloromethane using 0.100 M tetrabutylammonium tetrafluoroborate as supporting electrolytes, by potentiostat/galvanostat Autolab (PGASTAT 30) equipped with a standard three-electrode cell. A 2-mm-diameter GC was performed as the working electrode, a silver/silver chloride (Ag/AgCl) electrode as reference electrode and a platinum electrode was used as counter electrodes. electrochemical impedance spectroscopy (EIS) was performed in 5.0 mM $\text{K}_3[\text{Fe}(\text{CN})_6]/\text{K}_4[\text{Fe}(\text{CN})_6]$ solution. An AC voltage was applied with 5 mV amplitude in the frequency range of 0.01 Hz - 100 kHz. The thermogravimetric analysis (TGA) was performed by Perkin Elmer thermogravimetric analyzer at a heating rate of $10^\circ\text{C min}^{-1}$ from 25°C to 700°C under Ar atmosphere. DMTA analysis was performed using Mk IV DMTA instrument, Data were obtained at 10 hz, from -100 to 100°C and the heating rate was 2°C/min .

2.2. General procedure for the synthesis of 5-chloro-2,2-bis(alkylferrocenyl)pentane derivatives (2a, b)

2a and **2b** were prepared according to the procedure described in our previous report [50]. Briefly, a 25 ml two-necked round bottomed flask was equipped with an Ar inlet adapter and a magnetic stirrer. Dry methanol (3 ml), sulfuric acid (3 ml), alkylferrocene (16 mmol) (synthesized according to the procedure reported previously [51]) and 5-chloro-2-pentanone (8 mmol, 0.92 ml) were mixed and stirred at 65 °C under argon gas. After 30 h, the reaction mixture was cooled to ambient temperature and after neutralization with sodium carbonate. The mixture was extracted with dichloromethane (3 × 20 ml). Then the solvent was removed by rotary evaporator and 5-chloro-2,2-bis(alkylferrocenyl)pentane derivatives were purified by column chromatography using hexane as eluent.

2.2.1. 5-Chloro-2,2-bis(ethylferrocenyl)pentane (2a)

From 3.42 g of **1a**, 2.54 g (4.8 mmol) of the viscous orange oil was obtained with 60% yield; ¹H NMR (400 MHz, CDCl₃, δ): 4.01–3.91 (m, 16H, Fc), 3.45 (t, 2H, -CH₂Cl), 2.35–2.26 (m, 4H, -CH₂-Fc), 1.99–1.95 (m, 2H, -CH₂CH₂Cl), 1.67–1.55 (m, 5H, CH₃ and CH₂), 1.16 (t, 6H, CH₃CH₂-Fc); IR (KBr): ν = 3090 (w; C-H, Aromatic), 2971 (s; C-H, Aliphatic), 1638 (m; C=C), 645 (m; C-Cl), 485 (w; Fe-Cp) cm⁻¹; HRMS (ESI) m/z: 532 [M+2]⁺, 530 [M]⁺; calcd for C₂₉H₃₅ClFe₂: C 65.63%, H 6.64%, Fe 21.04%; found: C 65.67%, H 6.61%, Fe 21.03%.

2.2.2. 5-Chloro-2,2-bis(propylferrocenyl)pentane (2b)

From 3.65 g of **1b**, 2.59 g (4.64 mmol) of the high viscosity orange oil was obtained; yield 58%; ¹H NMR (400 MHz, CDCl₃, δ): 4.00–3.76 (m, 16H, Fc), 3.38 (t, 2H, -CH₂Cl), 2.24–2.10 (m, 4H, -CH₂-Fc), 1.94–1.82 (m, 2H, -CH₂CH₂Cl), 1.60–1.35 (m, 9H, CH₃, CH₂ and -CH₂CH₂-Fc), 0.84 (t, 6H, CH₃-propyl); IR (KBr): ν = 3084 (w; C-H, Aromatic), 2975 (s; C-H, Aliphatic), 1630 (m; C=C), 647 (m; C-Cl), 483 (w; Fe-Cp) cm⁻¹; HRMS (ESI) m/z: 560 [M+2]⁺, 558 [M]⁺; calcd for C₃₁H₃₉ClFe₂: C 66.63%, H 7.03%, Fe 19.99%; Found: C 66.59%, H 6.99%, Fe 19.94%.

2.3. General procedure for the synthesis of [4,4-bis(alkylferrocenyl)pentyl]dimethylsilane derivatives (3a, b)

3a and **3b** were prepared according to the procedure described by our team [51]. Briefly, a 25 ml round bottomed flask was equipped with an argon inlet adapter and magnetic stirrer. 5-chloro-2,2-bis(alkylferrocenyl)pentane (**2a, b**) (3 mmol) dissolved in dry THF (8 ml). Then 2 ml of the mentioned solution was added to 1 mL dry THF containing magnesium turnings (0.072 g, 3 mmol) and a large Iodine crystal, then this mixture was stirred at room temperature until the initial reaction was commenced (approximately 5 min). After that, the remaining of THF solution containing 5-chloro-2,2-bis(alkylferrocenyl)pentane (**2a, b**) was added slowly to the reaction mixture via a dropping funnel for 5 min. The mixture was refluxed under argon gas until all the magnesium turnings dissolved. After completion of the dissolution, the reaction mixture was cooled to room temperature and was added dropwise to the solution of chlorodimethylsilane (0.28 g, 3 mmol) in dry THF (4 ml) via a dropping funnel in the period of 30 min. The reaction mixture was refluxed under argon gas for 5 h. After completion of the reaction, the solvent was removed and light brown oil of [4,4-bis(alkylferrocenyl)pentyl]dimethylsilane derivatives (**3a, b**) were obtained with column chromatography using hexane as eluent.

2.3.1. [4,4-Bis(ethylferrocenyl)pentyl]dimethylsilane (3a)

From 1.59 g of **2a**, 1.44 g (2.73 mmol) of the light brown oil was obtained; yield 91%; ¹H NMR (400 MHz, CDCl₃, δ):

4.08–3.90 (m, 16H, Fc), 2.35–2.26 (m, 4H, -CH₂-Fc), 1.83–1.81 (m, 2H, -CH₂CH₂Si(Me)₂H), 1.62–1.55 (m, 5H, CH₃ and CH₂), 1.15 (t, 6H, CH₃CH₂-Fc), 0.53 (t, 2H, -CH₂Si(Me)₂H), 0.049–0.043 (m, 6H, Si(CH₃)₂H); IR (KBr): ν = 3020 (w; C-H, Aromatic), 2926 (s; C-H, Aliphatic), 2107 (w; Si-H), 1636 (m; C=C), 1255 (s; Si-C), 485 (w; Fe-Cp) cm⁻¹; HRMS (ESI) m/z: 554 [M]⁺; calcd for C₃₁H₄₂Fe₂Si: C 67.16%, H 7.63%, Fe 20.15%; Found: C 67.11%, H 7.59%, Fe 20.13%.

2.3.2. [4,4-Bis(propylferrocenyl)pentyl]dimethylsilane (3b)

From 1.67 g of **2b**, 1.63 g (2.64 mmol) of the light brown oil was obtained; yield 88%; ¹H NMR (400 MHz, CDCl₃, δ): 3.99–3.77 (m, 16H, Fc), 2.22–2.12 (m, 4H, -CH₂-Fc), 1.79–1.69 (m, 2H, -CH₂CH₂Si(Me)₂H), 1.56–1.36 (m, 9H, CH₃, CH₂ and -CH₂CH₂-Fc), 0.85 (t, 6H, CH₃-propyl), 0.75 (t, 2H, -CH₂Si(Me)₂H), 0.14–0.01 (m, 6H, Si(CH₃)₂H); IR (KBr): ν = 3022 (w; C-H, Aromatic), 2928 (s; C-H, Aliphatic), 2112 (w; Si-H), 1635 (m; C=C), 1258 (s; Si-C), 489 (w; Fe-Cp) cm⁻¹; HRMS (ESI) m/z: 582 [M]⁺; calcd for C₃₃H₄₆Fe₂Si: C 68.05%, H 7.96%, Fe 19.17%; Found: C 68.09%, H 7.91%, Fe 19.15%.

2.4. General procedure for the synthesis of [4,4-bis(alkylferrocenyl)pentyl]dimethylsilane grafted HTPB derivatives (4)

A 100 ml round bottomed flask was equipped with an argon inlet adapter and magnetic stirrer. A mixture of the required amounts (Weight %) of [4,4-bis(alkylferrocenyl)pentyl]dimethylsilane (**3a, b**), and hydroxyl terminated poly butadiene (HTPB), was dissolved in hexane (50 ml) and hexachloroplatinic acid (H₂PtCl₆) was added as catalyst (0.05 ml of 0.01 M in 2-propanol). The reaction mixture was refluxed until the Si-H peak in the IR spectrum (near 2110 cm⁻¹) was eliminated. After completion of the reaction, the mixture was cooled to room temperature, filtered to remove the Pt-catalyst and solvent was removed by a rotary evaporator. The residue was placed on 3–5 cm silicagel and washed with hexane to remove the unreacted reactants. Finally, by washing the silicagel using EtOAc, viscous dark brown oil of [4,4-bis(alkylferrocenyl)pentyl]dimethylsilane grafted HTPB derivatives was obtained.

2.4.1. [4,4-Bis(ethylferrocenyl)pentyl]dimethylsilane grafted HTPB containing 8.59% of Fe (4a)

Using 0.20 g (0.36 mmol) of **3a** and 0.26 g of HTPB, **4a** was obtained as viscous dark brown oil.

2.4.2. [4,4-Bis(ethylferrocenyl)pentyl]dimethylsilane grafted HTPB containing 11.82% of Fe (4a')

Using 0.20 g (0.36 mmol) of **3a** and 0.14 g of HTPB, **4a'** was obtained as viscous dark brown oil.

2.4.3. [4,4-Bis(ethylferrocenyl)pentyl]dimethylsilane grafted HTPB containing 15.98% of Fe (4a'')

Using 0.20 g (0.36 mmol) of **3a** and 0.05 g of HTPB, **4a''** was obtained as viscous dark brown oil; ¹H NMR (400 MHz, CDCl₃, δ): 5.57–4.91 (m, -C=CH, -C=CH₂ of HTPB), 4.15–3.90 (m, 16H, Fc), 2.31–2.29 (m, 4H, -CH₂-Fc), 2.07–2.02 (m, -CH₂, Aliphatic of HTPB), 1.67–1.57 (m, 5H, CH₃ and CH₂), 1.19 (t, 6H, CH₃CH₂-Fc), 0.91–0.85 (t, 2H, CH₂-Si), 0.09–0.05 (d, 6H, -Si(CH₃)₂-); IR (KBr): ν = 3410 (br; -OH), 3073 (s; C-H, Aromatic), 2919 (s; C-H, Aliphatic), 1642 (m; C=C), 1257 (s; Si-C), 474 (w; Fe-Cp) cm⁻¹.

2.4.4. [4,4-Bis(propylferrocenyl)pentyl]dimethylsilane grafted HTPB containing 8.12% of Fe (4b)

Using 0.21 g (0.36 mmol) of **3b** and 0.28 g of HTPB, **4b** was obtained as viscous dark brown oil.

2.4.5. [4,4-Bis(propylferrocenyl)pentyl]dimethylsilane grafted HTPB containing 11.23% of Fe (**4b'**)

Using 0.21 g (0.36 mmol) of **3b** and 0.14 mg of HTPB, **4b'** was obtained as viscous dark brown oil.

2.4.6. [4,4-Bis(propylferrocenyl)pentyl]dimethylsilane grafted HTPB containing 15.01% of Fe (**4b''**)

Using 0.21 g (0.36 mmol) of **3b** and 0.05 g of HTPB, **4b''** was obtained as viscous dark brown oil; ^1H NMR (400 MHz, CDCl_3 , δ): 5.58–4.84 (m, $-\text{C}=\text{CH}_2$, $-\text{C}=\text{CH}_2$ of HTPB), 4.02–3.82 (m, 16H, Fc), 2.30–2.28 (m, 4H, $-\text{CH}_2\text{-Fc}$), 2.00–1.96 (m, $-\text{CH}_2$, Aliphatic of HTPB), 1.56–1.36 (m, 9H, CH_3 , CH_2 and $-\text{CH}_2\text{CH}_2\text{-Fc}$), 0.85–0.75 (m, 8H, $\text{CH}_2\text{-Si}$ and $\text{CH}_3\text{-propyl}$), 0.07–0.01 (d, 6H, $-\text{Si}(\text{CH}_3)_2$); IR (KBr): $\nu = 3564$ (br; $-\text{OH}$), 3012 (w; C–H, Aromatic), 2921 (s; C–H, Aliphatic), 1645 (m; C=C), 1262 (s; Si–C), 483 (w; Fe–Cp) cm^{-1} .

2.5. Preparation of modified electrode

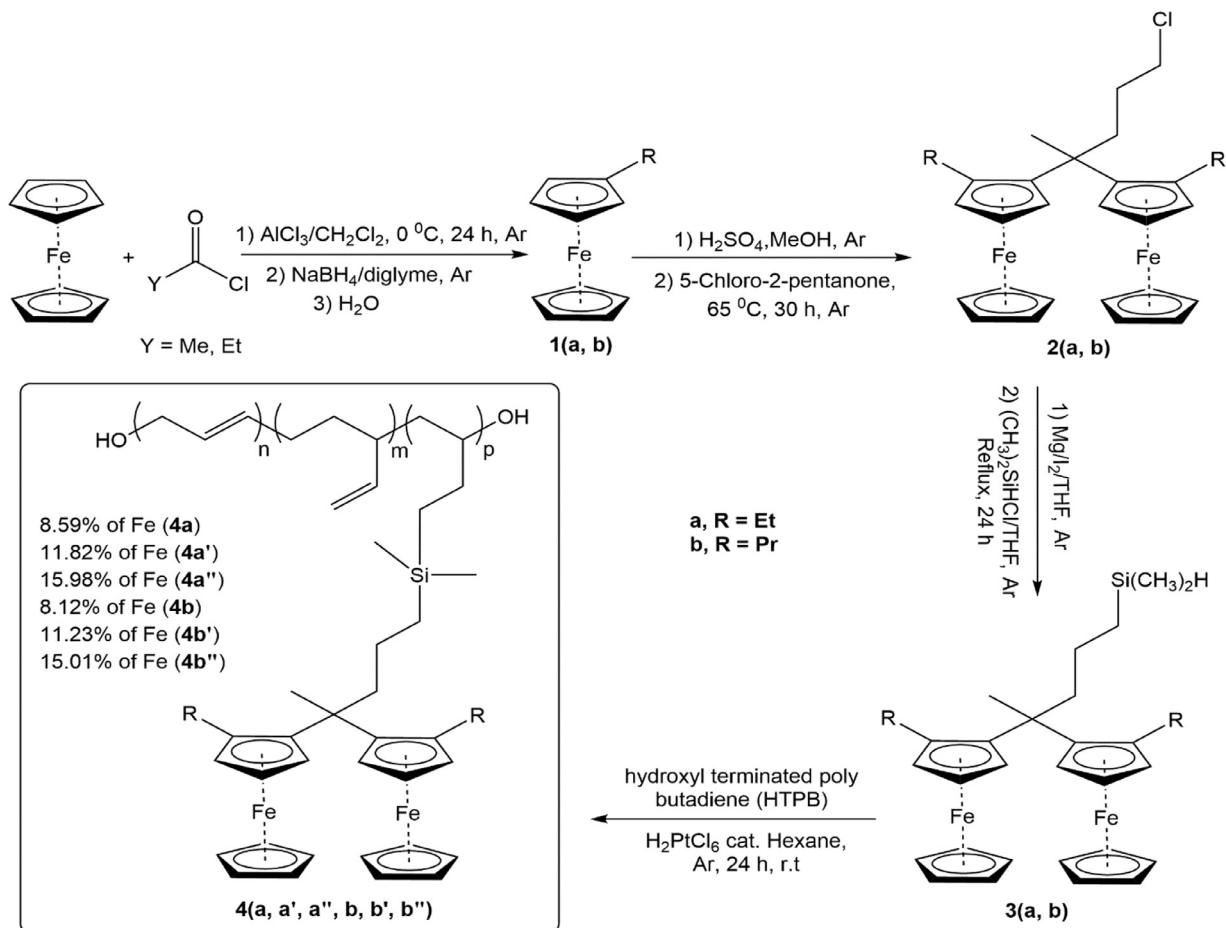
Initially, the GC electrode was polished using alumina, sonicated in H_2SO_4 (2N), and distilled water, sequentially. When the well-defined stable cyclic voltammogram was obtained for scanning of GCE treatment in H_2SO_4 (2N) at the range of -1 to 1 V, the electrode became ready for surface modification. For this purpose, the 10% CH_2Cl_2 solution of terephthalaldehyde (TFA) and 10% CH_2Cl_2 solution of fresh egg white (FEW) was added to 5 mg of as-synthesized ferrocene containing polymer (BEFcHTPB) which was dissolved in CH_2Cl_2 . The Obtained suspension was sonicated for 10 min to form the homogenous BEFcHTPB/(TFA+FEW) complex. Finally, with drop-coating of obtained complex (5 μl) on GCE sur-

face, the GC/BEFcHTPB/(TFA+FEW) was prepared as the modified electrode.

3. Results and discussion

3.1. Design and preparation of modified polymers

Scheme 1 illustrated the synthesis of [4,4-bis(alkylferrocenyl)pentyl]dimethylsilane derivatives Grafted HTPB via the facile method and acceptable yields. As the starting point, alkylferrocene derivatives (Ethyl and Propyl) were prepared via Friedel-Crafts acylation followed by reduction of the acylated ferrocenes to alkyl derivatives [51]. Then the obtained alkylferrocenes (**1a**, **b**) reacted with 5-chloro-2-pentanone according to the condensation reaction method described in our previous report [50] in order to attain 5-chloro-2,2-bis(alkylferrocenyl)pentane derivatives (**2a**, **b**). Since 5-chloro-2,2-bis(alkylferrocenyl)pentane lacks a suitable functional group for the HTPB polymer framework grafting, the conversion of the chlorine to dimethylhydrosilyl group was done through Grignard reaction. For this purpose, Grignard reagent was prepared *in situ* by adding bis-alkylferrocene containing chloropentane derivatives (**2a**, **b**) to magnesium turnings in dry THF. The Obtained mixture was reacted with chlorodimethylsilane and resulted in the formation of ethyl and propyl substituted [4,4-bis(alkylferrocenyl)pentyl]dimethylsilane derivatives (**3a**, **b**) with 91 and 88% yields, respectively. Finally, hydrosilylation reaction of bis-alkylferrocenesilane and HTPB in the presence of hexachloroplatinic acid (H_2PtCl_6) as catalyst and hexane as solvent



Scheme 1. Synthesis of [4,4-bis(alkylferrocenyl)pentyl]dimethylsilane modified derivatives of Grafted HTPBs.

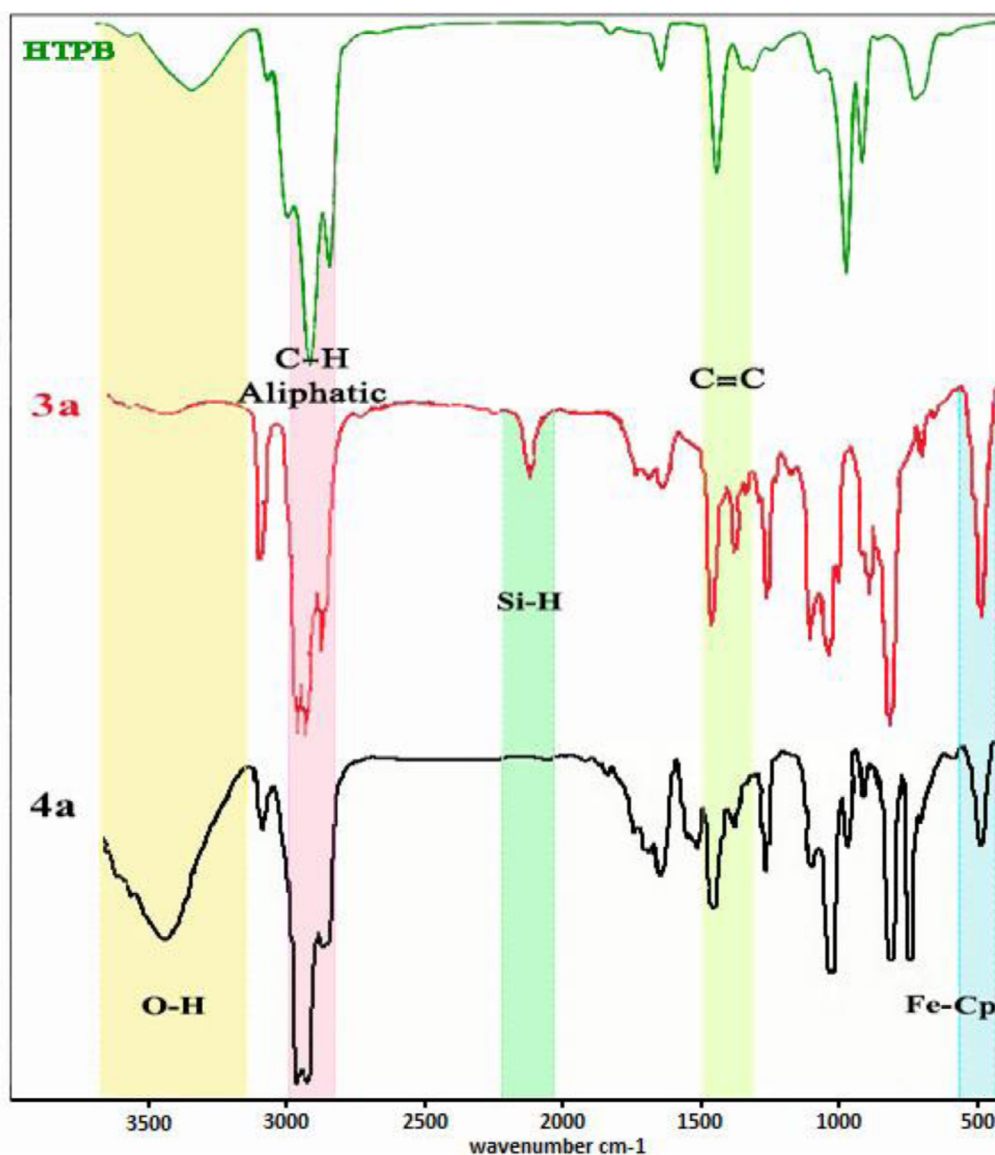


Fig. 1. FT-IR spectra of HTPB, silane derivative (3a) and final polymer (4a).

finished with the synthesise of the modified electroactive HTPB polymers **4** with high Iron percent (Fe %).

3.2. Spectroscopy studies

FT-IR spectroscopy was used to monitor the elimination of the Si-H absorption peak at approximately 2110 cm^{-1} (Fig. 1), which confirms that the silane compounds were grafted to HTPB backbone successfully. On average, it takes 24 h to complete the reaction. Fig. 2 depicts the thin layer chromatography (TLC) plate which was developed in hexane:EtOAc (8:2) as eluent, then the plate was dried and sprayed with a 50% v/v aqueous solution of sulfuric acid in a fume hood in order to manifest the pristine HTPB. As can be seen the final polymer with $R_f = 0.5$ was completely separated from the ferrocenylsilane ($R_f = 0.83$) and pristine HTPB ($R_f = 0.16$). On the other hand; in primary plate **A** the pristine HTPB was not detectable, while the final polymer was perfectly visible with the naked eye due to the attachment of the chromophore groups (ferrocene).

Because of the grafting of ferrocenyl nucleus to polymer skeleton which cannot apply a perceptible effect on the size and dis-

persity of polymer, gel permeation chromatography (GPC) was not a suitable method for the characterization of this type of polymers. The atomic absorption spectroscopy was used for the determination of iron percentage in final polymers. HTPB polymer is a macromolecule composed of many repeated subunits with C=C bond. The molecular weight of these repeated units is 54 amu. Meanwhile the molecular weights of alkylferrocenylsilanes are 554 and 582 amu for ethyl (3a) and propyl (3b) derivatives, respectively. Therefore, the HTPB polymer is capable of ferrocenylsilane loading. The variation of Fe content in the grafted polymer is obtained by simply making changes in the mole ratio of the HTPB and the ferrocene derivatives. The catalyst content is constant for all experiments, since the amount of starting material used in this study is not very variable (0.05–0.26 g) because it requires a change in the catalyst value. The used amount of catalyst is surplus. The mole ratio of C=C bond and Si-H units used in HTPB and ferrocenyl derivatives in each reaction were assembled in Table 2.

The comparison of pristine HTPB and ferrocenylsilane FT-IR spectra with final polymer indicates the introducing of ferrocenyl units to polymer backbones. As can be seen in comparative Table 3, in the final polymer the distinct peaks of HTPB are visible as

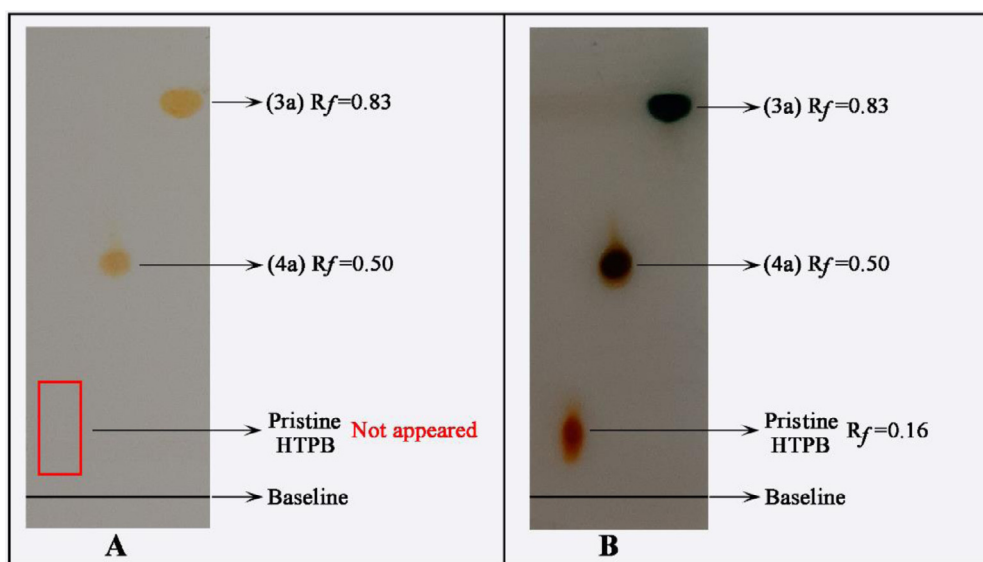


Fig. 2. TLC plate for pristine HTPB, **3a** and **4a**, A) primary plate, B) after spraying with sulfuric acid.

Table 2

Comparison between the mol ratio of C=C bond and Si-H units.

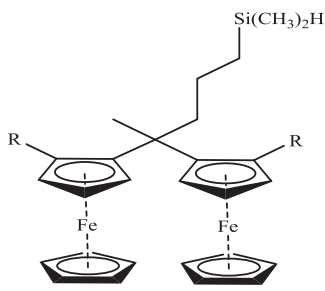
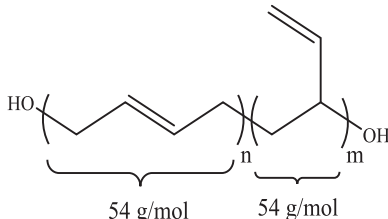
 <p>R=Et (3a), $M_W=554$ g/mol R=Pr (3b), $M_W=582$ g/mol</p>	 <p>54 g/mol 54 g/mol</p>	<p>Molar ratio mol C=C in HTPB mol Si-H 3a or 3b</p>	
0.20 g (0.36 mmol) of 3a is equal to 0.36 mmol Si-H bond	0.26 g of HTPB is equal to 4.78 mmol C=C bond		13.27
0.20 g (0.36 mmol) of 3a is equal to 0.36 mmol Si-H bond	0.14 g of HTPB is equal to 2.57 mmol C=C bond		7.14
0.20 g (0.36 mmol) of 3a is equal to 0.36 mmol Si-H bond	0.05 g of HTPB is equal to 0.92 mmol C=C bond		2.55
0.21 g (0.36 mmol) of 3b is equal to 0.36 mmol Si-H bond	0.28 g of HTPB is equal to 5.15 mmol C=C bond		14.30
0.21 g (0.36 mmol) of 3b is equal to 0.36 mmol Si-H bond	0.14 g of HTPB is equal to 2.57 mmol C=C bond		7.14
0.21 g (0.36 mmol) of 3b is equal to 0.36 mmol Si-H bond	0.05 g of HTPB is equal to 0.92 mmol C=C bond		2.55

Table 3

IR peak signature of pristine HTPB, **3a** and **4a** compounds.

HTPB	3a	4a
3345 (-OH)	-	3342 (-OH)
-	3022 (-CH aromatic)	3032 (-CH aromatic)
2917 (-CH aliphatic)	2928 (-CH aliphatic)	2925 (-CH aliphatic)
969-1310 (-CH)	1258 (C-Si)	1262 (C-Si)
1440-1643 (C=C)	481 (C-Fe)	481 (C-Fe)
-	2112 (Si-H)	Disappeared

well as ferrocenylsilane peaks. Additionally, ^1H -NMR spectra can also be used for this purpose. In the ^1H NMR spectra of final polymer, the $-\text{CH}_2$ and the peaks for unreacted vinyl groups of HTPB can be seen along with the indicative ferrocene peaks, which confirms the modification of pristine HTPB with ferrocenylsilane. Bis alkylferrocene-grafted hydroxyl terminated polybutadiene [(alkylFc) $_2$ -HTPB], exhibits two sharp resonances for the two sets of cyclopentadienyl protons at 3.90-4.15 ppm and the proton resonance from $(\text{CH}_3)_2\text{Si}-$ is visible at 0.05-0.09 ppm (Fig. 3). The

introduction of these peaks to ^1H -NMR spectra of the final polymers, confirms the ferrocene functionalization of HTPB.

3.3. Physical properties of synthesized polymers

In continue, we investigated the physical properties such as iron percentage, hydroxyl value, viscosity and glass transition temperature for modified polymers, and compared them with alkylbutadienes which reported in our previous work [47,48]. Results are summarized in Table 4.

The iron percentage of the modified polymers was measured using atomic absorption spectrophotometer in the range of 8-16 wt%. These values are significant compared to that of alkylbutadienes, since in this research bis-nuclear ferrocenyl derivatives were used as modifying agents. Obviously, with increasing the grafting of ferrocene moiety, the iron content of final polymer showed increases as well.

Studies showed that the viscosity of such polymers is affected by two different factors: 1) Viscosity increased with increasing iron content, 2) viscosity decreased with increasing the length of alkyl

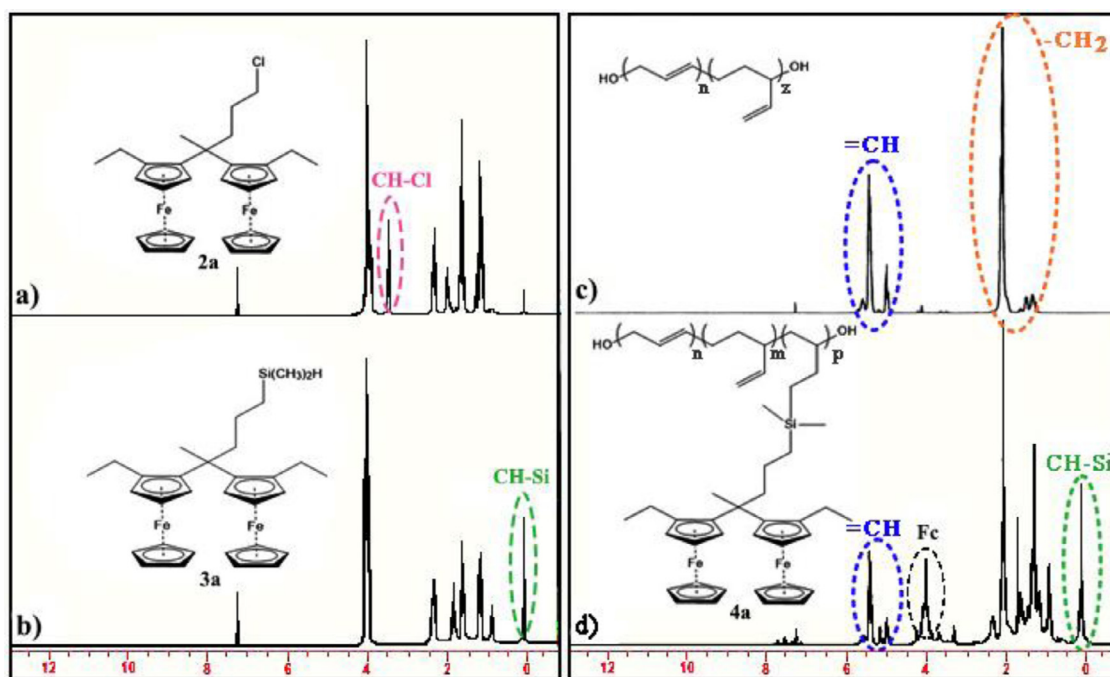


Fig. 3. ^1H NMR spectra of **2a**, **3a** and **4a** as representative of synthesized compounds.

Table 4

Iron percentage, viscosity, glass transition temperature and hydroxyl value for HTPB and alkyl Fc-HTPB derivatives.

Entry	Compound	Iron content (%)	Viscosity (Pa.s)	Glass transition temperature ($^{\circ}\text{C}$)	Hydroxy Value (mmol OH/g)
1	HTPB ^a	-	3.4	-73.2	0.8
2	Ethyl Fc-HTPB ^a	3.16	3.92	-70.8	-
3	Ethyl Fc-HTPB ^a	8.2	4.48	-68.4	-
4	Ethyl Fc-HTPB ^a	9.2	5.13	-64.3	-
5	4a	8.59	4.68	-67.9	0.46
6	4a'	11.82	5.43	-64.4	0.33
7	4a''	15.98	6.23	-61.5	0.16
8	Propyl Fc-HTPB ^a	5.9	3.62	-72.4	-
9	Propyl Fc-HTPB ^a	8.2	4.26	-71.5	-
10	Propyl Fc-HTPB ^a	10.27	4.98	-70.1	-
11	4b	8.12	4.37	-67.1	0.48
12	4b'	11.23	5.14	-63.8	0.34
13	4b''	15.01	5.83	-60.7	0.17

^a Reference [47].

branch on the ferrocene core. According to the mentioned points, these polymers have a relatively higher viscosity compared with similar alkylbutacenes which accounts for a high iron content. On the other hand, greater extent of side branching substituents in these polymers caused a decrease in viscosity values in comparison to polymers of the same iron percentage. As can be seen in Table 4, the viscosity value in [4,4-bis(ethylferrocenyl)pentyl]dimethylsilane grafted HTPB derivatives is higher than that of propyl derivatives. Although this difference is very small, it is recognizable.

The hydroxyl content of HTPB and all modified polymers were determined by acetylation with excess acetic anhydride followed by back-titration with standard alcoholic KOH [45]. Obtained results were listed in Table 4. Hydroxyl values decreased with increasing of iron content in the modified polymers. Obviously, OH groups are constant, while a large number of alkylferrocenylsilane molecules are linked per unit of the polymer. Hydroxyl terminated groups of pristine HTPB remained intact in the modified HTPB after hydrosilylation reaction.

Fig. 4(a) shows the plot of iron content versus viscosity for synthesized polymers, this figure obviously shows increasing of the iron content and decreasing in the length of side chain result in the viscosity increasing. We report results of glass transition temperatures (T_g) measurements for modified polymers ranging from about -67.9°C to about -60.7°C . Fig. 4(b) clearly shows the proportion between the glass transition temperature and iron content of modified polymers. The T_g values are directly related to the iron percentage of polymer which reflects the number of grafting ferrocenes. In contrast, the glass transition temperature tangibly starts to decrease with an increasing in the number of carbons in the substituted groups.

3.4. Thermal properties

The dynamic mechanical thermal analysis (DMTA) was used for measuring glass transition temperature of prepared polymers, the $\tan \delta$ as a function of temperature for all of the final ferrocenyl

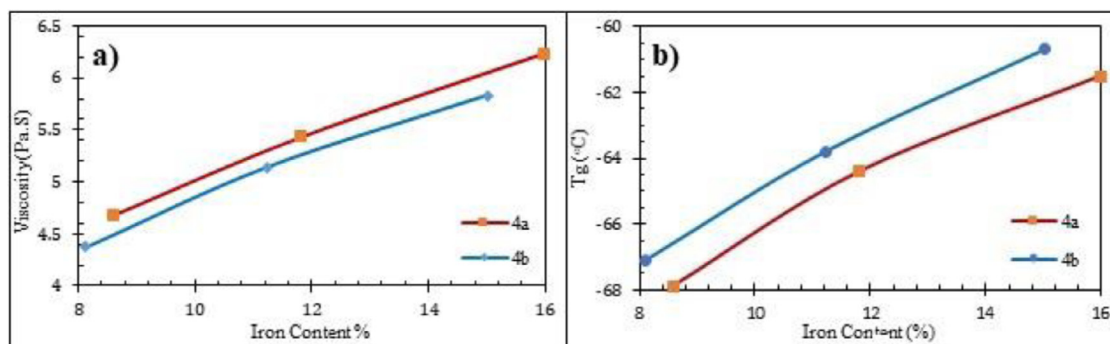


Fig. 4. Plot of (a) the iron content versus the viscosity and (b) the iron content versus glass transition temperature for modified polymers.

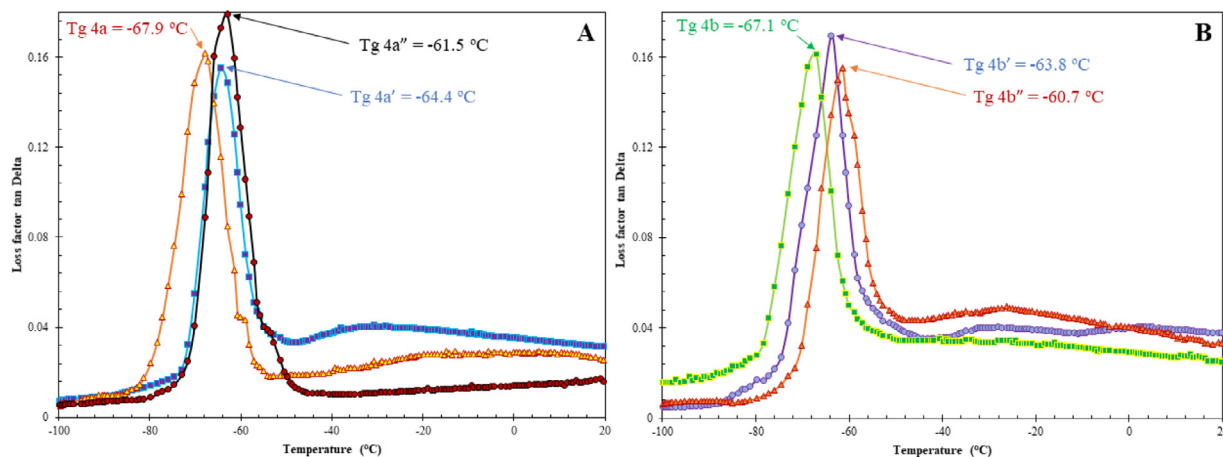


Fig. 5. The DMTA plot for (A) ethylferrocene and (B) propylferrocene derivatives grafted HTPB.

modified polymers is shown in Fig. 5. In synthetic polymers the position of the $\tan \delta$ peak was considered as glass transition temperature. As previously stated, the glass transition temperature and iron content of modified polymers have a direct relationship. On the other hand, the increase in the number of carbons (ethyl to propyl) led to a slight decrease in glass transition temperature.

The TGA thermograms of final polymers, are illustrated in Fig. 6. The thermal degradation profile for all of the ferrocenyl modified polymers in this work contain the three-stage weight loss process. At first, the little weight loss (6–7%) can be related to the water removal of samples. In continue, thermal decomposition of polymers is detectable with significant weight loss in ≤ 500 °C. Finally, after heating the polymer samples up to 700 °C, Fe residual as a percentage of the sample total weigh was remained, which is in good agreement with atomic absorption data for iron percentage.

3.5. Optical properties

Ferrocenyl compounds display unique optical properties, ferrocene units in the main chain of polymer create optical properties in the modified HTPB. Fig. 7 shows the UV-vis spectra of the prepared ferrocenyl modified polymers. As shown in Fig. 7 there are two characteristic transitions (λ_{\max}), the overall value of lower wavelengths is approximately 320 nm which is assigned to π - π^* transition of ferrocenyl cyclopentadienyl ring and the second one is located in 440 to 460 nm, this absorption is due to metal-to-ligand charge transfer (MLCT). As expected, the absorption intensity is influenced by the sample iron percentage, which means the intensity of absorption increases with an increase in the ferrocenyl grafting to HTPB polymer.

Table 5

Selected electrochemical data for the synthesized polymers in DCM/0.100 M (Bu)₄N.BF₄ at 25.0 °C.

Entry	compound	Ep _a	Ep _c	ΔE	I _c /I _a
1	4a	0.6738	0.4150	0.2588	0.5219
2	4a'	0.6787	0.4196	0.2591	0.6187
3	4a''	0.6790	0.4004	0.2786	0.5897
4	4b	0.7666	0.4248	0.3418	0.5843
5	4b'	0.7715	0.4346	0.3369	0.4484
6	4b''	0.7764	0.4395	0.3369	0.3791

3.6. Electrochemical properties of modified polymers

In order to investigate the electrochemical properties of synthesized polymers, cyclic voltammetry was performed in dichloromethane with 0.1 M tetrabutylammonium tetrafluoroborate as supporting electrolyte. Electrochemical data summarized in Table 5 and Fig. 8 depicts the CV curves for all polymers, an obvious redox peak is assigned to the Fc/Fc⁺ system. As can be seen in Fig. 8a and 8e by increasing the iron content, peak currents increase. Obtained results are in agreement with the atomic absorption data and higher peak currents indicate higher ferrocenyl grafting since ferrocene is the electroactive group in final polymers. Fig. 8d and 8h compare the CV diagrams of mono and bis-nuclear ferrocene grafting polymers, and the obtained results are in line with other data and corroborating the increase in ferrocene linkage to the HTPB framework. Furthermore, the effect of scan rate on peak current was studied in the same condition in the range of 25–200 mVs⁻¹ (Fig. 8b and 8f), the linear relationship with 0.99 regression coefficient was obtained via plotting of anodic and cathodic currents versus the square root of scan rates (Fig. 8c and

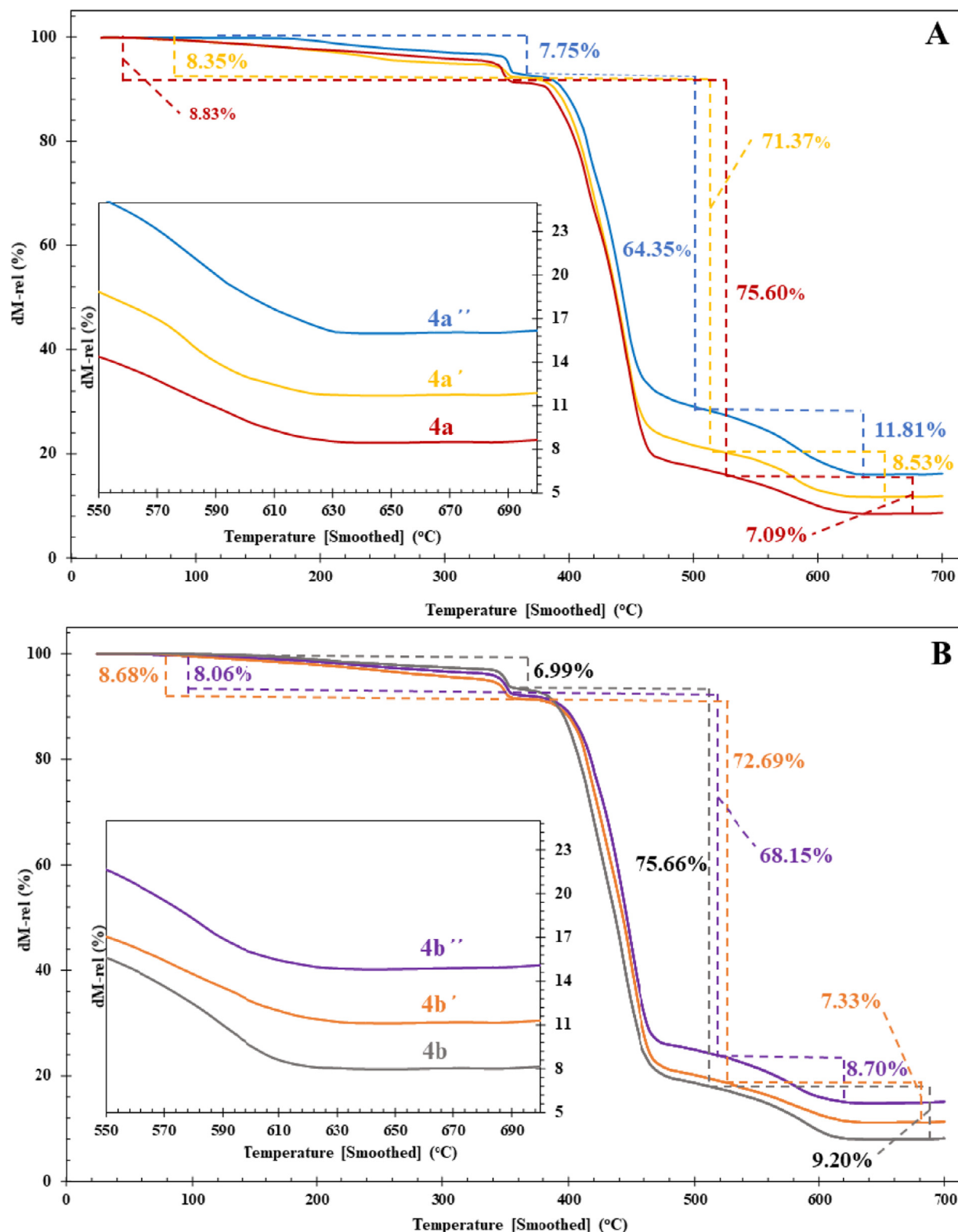


Fig. 6. TGA thermograms of (A) ethylferrocene and (B) propylferrocene derivatives grafted HTPB.

8g). This behavior suggests a diffusion-limited characteristic for the redox process.

3.7. Preparation of the modified electrode (GC/BEFCHTPB/(TFA+FEW))

In continue, the electrochemical behavior of the synthesized polymers was evaluated on the surface of GCE. For this pur-

pose, [4,4-Bis(ethylferrocenyl)pentyl]dimethylsilane grafted HTPB containing 15.98% of Fe (**4a''**) was chosen as representative of the final ferrocenyl polymers and abbreviated as BEFCHTPB. Since the appearance of all synthesized ferrocenyl polymers was viscous oil, it was impossible to dry them on the GCE surface to do electrochemical evaluations. Therefore, terephthaldehyde (TFA): a two

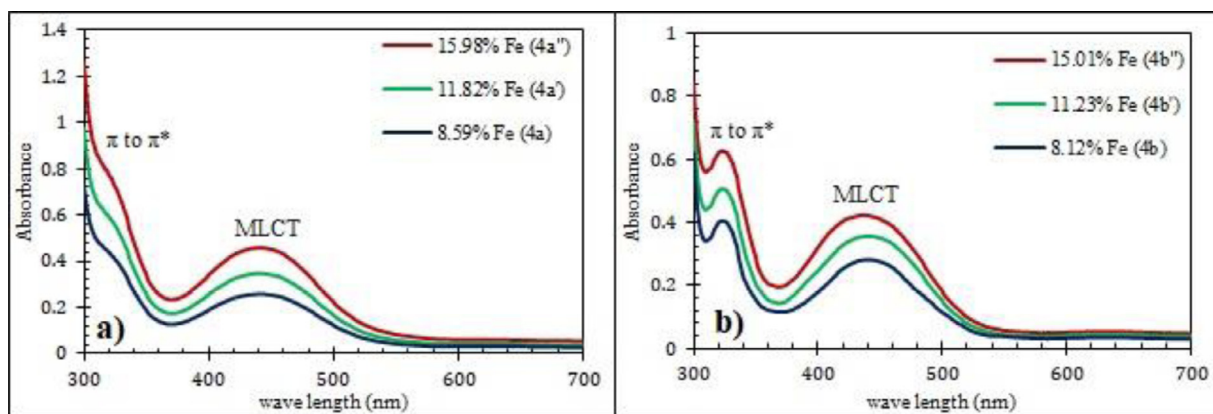


Fig. 7. UV-vis spectra of bis-ferrocenyl modified HTPB.

functional aldehyde and fresh egg white (FEW): a known and low cost protein as the cross-linking agent were used [52,53]. At first, the GC electrode was polished using alumina, sonicated in H_2SO_4 (2N), and distilled water, and scanned at the range of -1 to 1 V in H_2SO_4 (2N) until the well-defined stable cyclic voltammogram was observed. In continue, the 10% CH_2Cl_2 solution of TFA and 10% CH_2Cl_2 solution of FEW were added to 5 mg of BEFcHTPB which dissolved in dichloromethane. The final suspension was sonicated for 10 min and the homogenous BEFcHTPB/(TFA+FEW) complex was obtained. The GC/BECfHTPB/(TFA+FEW) modified electrode was fabricated by drop-coating of the obtained complex on the GCE surface.

3.8. Morphology study of the modified electrode

For morphology studies of GCE and GC/BECfHTPB/(TFA+FEW) modified electrode, the Field Emission Scanning Electron Microscopy (FE-SEM) technique was used. Fig. 9 depicts the related images at 2 μm magnification, the wrinkled surface of GCE after drop-coating with BEFcHTPB/(TFA+FEW) complex in comparison with the uniform structure of the bare GCE demonstrated the successful modification of GCE.

3.9. Interface properties of GC/BECfHTPB/(TFA+FEW)

Fig. 10 illustrated the Nyquist plots of bare GC and GC/BECfHTPB/(TFA+FEW) modified electrode measured in 5 mM $\text{K}_3[\text{Fe}(\text{CN})_6]/\text{K}_4[\text{Fe}(\text{CN})_6]$ solution, to study the interface properties. The faradaic electron-transfer was reflected in a semicircle at high frequencies as well as diffusional processes which can be shown a with linear line at low frequencies [54]. The successful immobilization of the BEFcHTPB/(TFA+FEW) complex on the bare GCE surface was demonstrated by a larger diameter of the semicircle in the Nyquist plot of GC/BECfHTPB/(TFA+FEW) modified electrode comparison to bare GC electrode. The semicircle diameter is related to charge transfer resistance (R_{ct}); with immobilization of BEFcHTPB/(TFA+FEW) complex on the GCE surface, the decrease in electrode conductivity led to increasing in charge transfer resistance.

3.10. DPV study of the prepared electrode for the capability of dopamine detection

FcHTPB/(TFA+FEW) complex, the fabricated electrode was scanned in the phosphate buffer solution (PBS) using a scan rate of 50 mV s^{-1} at the range of 0 to 1 V (Fig. 11a, red line), the

oxidation and reduction peaks of Fc/Fc^+ couple is quite obvious. Aiming to evaluate the modified electrode capability for dopamine determination, the fabricated electrode was scanned in the phosphate buffer solution (PBS) which spiked with 1mM dopamine under the same condition (Fig. 11a, blue line). As can be seen, the increase in peak current approves the sensitivity of fabricated electrode to dopamine. As mentioned in the literature dopamine can be oxidized through a two-electron and two-proton change process [55], and ferrocene can mediate the oxidation of dopamine. Fig. 12 shows the electrocatalytic dopamine oxidation process in the surface of GC/BECfHTPB/(TFA+FEW) modified electrode. Differential pulse voltammetry (DPV) is another effective electrochemical method that has been extensively used for dopamine detection, DPV studies can provide improved selectivity compared to CV. The DVP voltammogram of GC/BECfHTPB/(TFA+FEW) electrode in absence and presence of dopamine (1 mM) at scan rate of 50 mV s^{-1} depicted in Fig. 11b. The sensitivity of GC/BECfHTPB/(TFA+FEW) modified electrode to dopamine is marked by an increase in peak intensity.

3.11. Effect of solution pH in dopamine detection

The effect of solution pH on the peak current of the DPV voltammogram has been studied at five constant pH levels between 4.0 and 8.0 using GC/BECfHTPB/(TFA+FEW) modified electrode in 0.1 M PBS at a scan rate of 50 mV s^{-1} . The maximum value of DPV peak current was obtained in pH = 7 (Fig. 13). Additionally, the potential of DA oxidation was plotted versus pH. As can be seen in Fig. 13c, the positive and negative shift of DA potential was observed with changing in pH values. The result is implying that the modified electrode surface is suitable for actively electrons transformation in the electrochemical redox reaction of DA.

3.12. Linear range of modified electrode in dopamine detection

After the confirmation of the electrochemical response of the GC/BECfHTPB/(TFA+FEW) modified electrode to dopamine, the relationship between dopamine concentration and the oxidation peak current was evaluated using CV technique in PBS 0.1 M at pH 7.0. As can be seen in Fig. 14 with increasing the dopamine concentration at the range of 3 to 125 μM , the oxidation peak current increased linearly. According to the calibrate curve, the linear regression equation is: $I_{pa}(\mu\text{A}) = 0.1567C_{DA}(\mu\text{M}) + 1.5613$, and the correlation coefficient is 0.9968. The detection limit ($3\sigma/m$) and quantitation limit ($10\sigma/m$), was obtained as 0.048 μM and

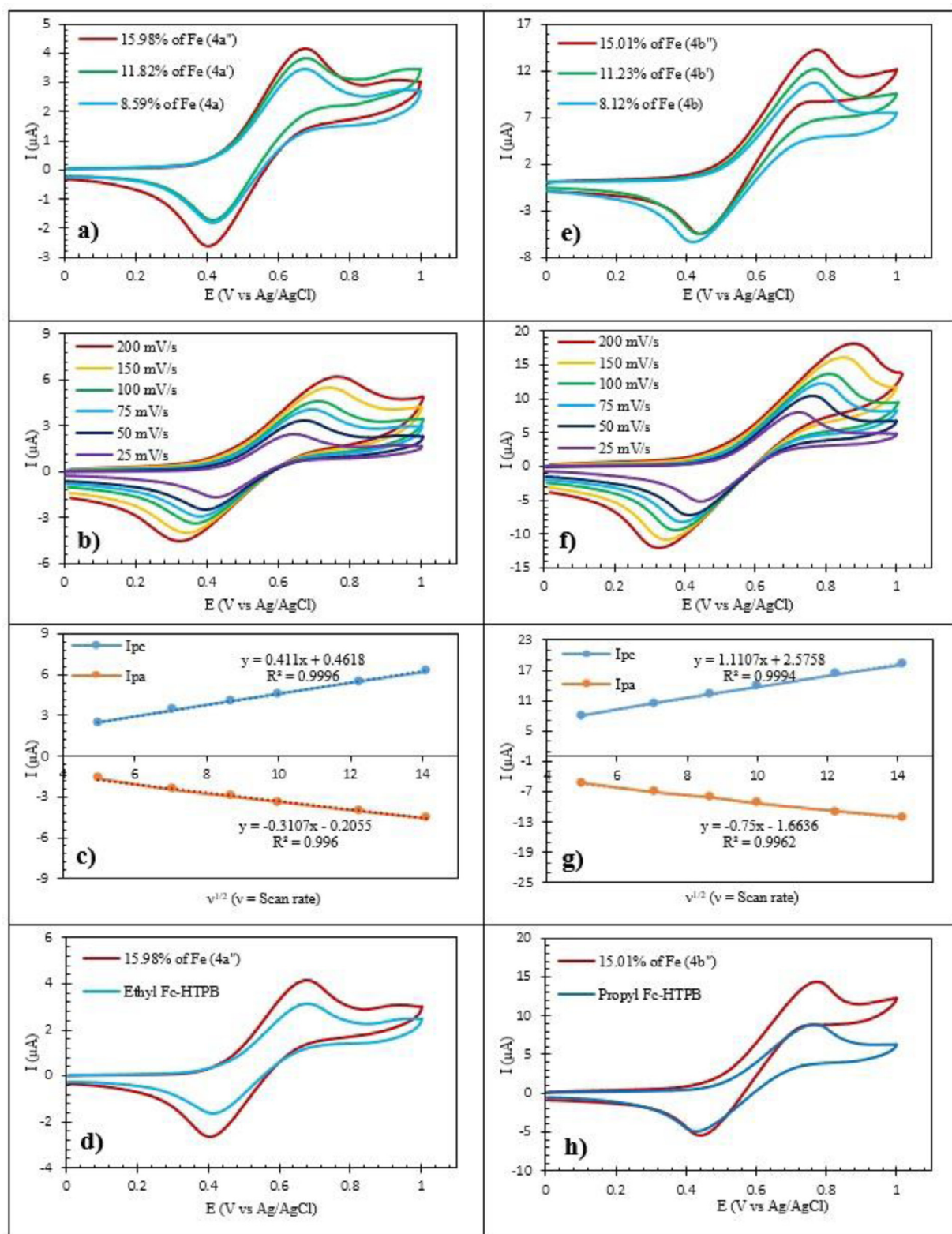


Fig. 8. Cyclic voltammetry plots for modified polymers (a) CV for ethyl derivatives with a variety of iron content, (b) CV curves of the 4a in different scan rates, (c) Linear relationship between the peak current and the square root of scan rates for 4a, (d) Comparison between CV curves of 4a and ethyl Fc-HTPB [48], (e) CV curves for propyl derivatives with variety of iron content, (f) CV curves of the 4b in different scan rates, (g) Linear relationship between the peak current and the square root of scan rates for 4b, (h) Comparison between CV curves of 4b and ethyl Fc-HTPB [48].

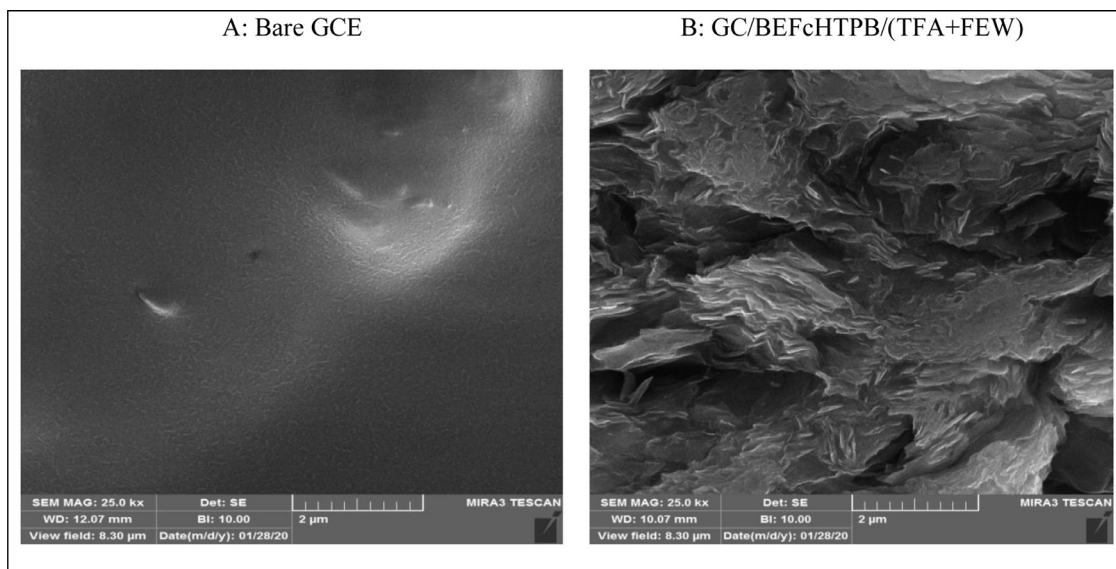


Fig. 9. SEM image of A: Bare GCE, and B: GC/BEFcHTPB/(TFA+FEW).

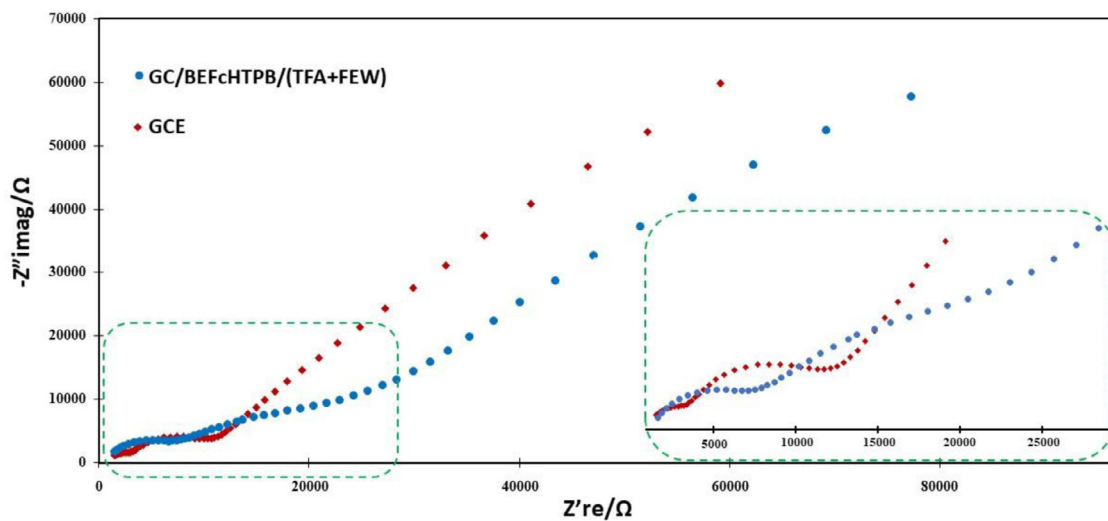


Fig. 10. The Nyquist curves of Bare GCE, and GC/BEFcHTPB/(TFA+FEW) modified electrode.

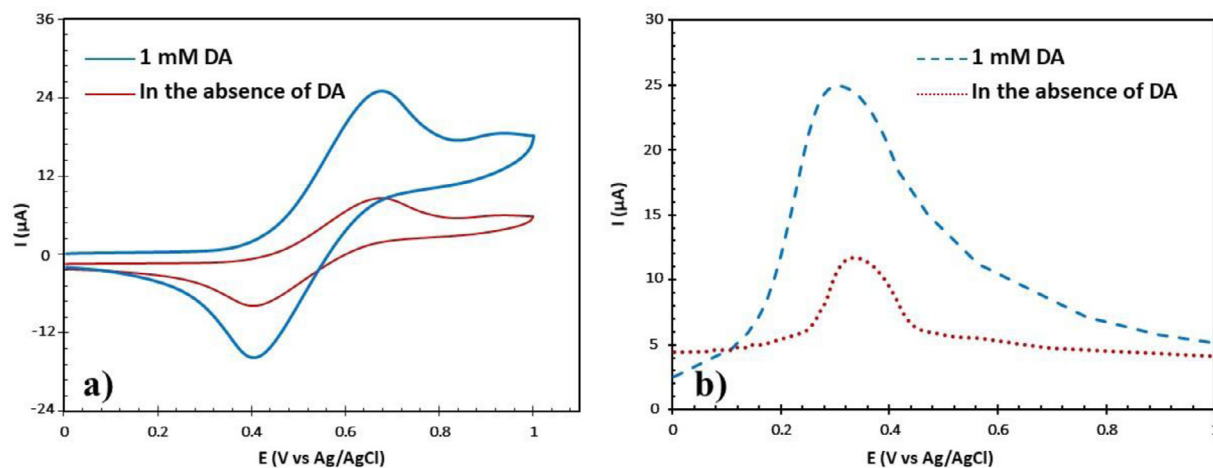


Fig. 11. (a) CV curves and (b) DPV voltammograms of GC/BEFcHTPB/(TFA+FEW) electrode in absence and presence of Dopamine. Scan rate: 50 mV s^{-1} .

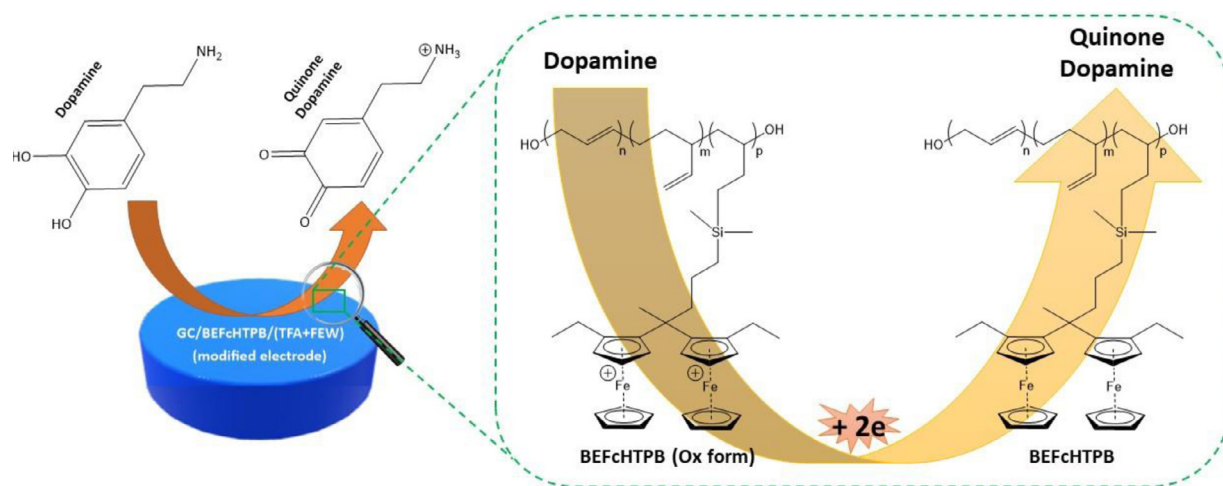


Fig. 12. The electrocatalytic dopamine oxidation process in the surface of GC/BEFchTPB/(TFA+FEW) modified electrode.

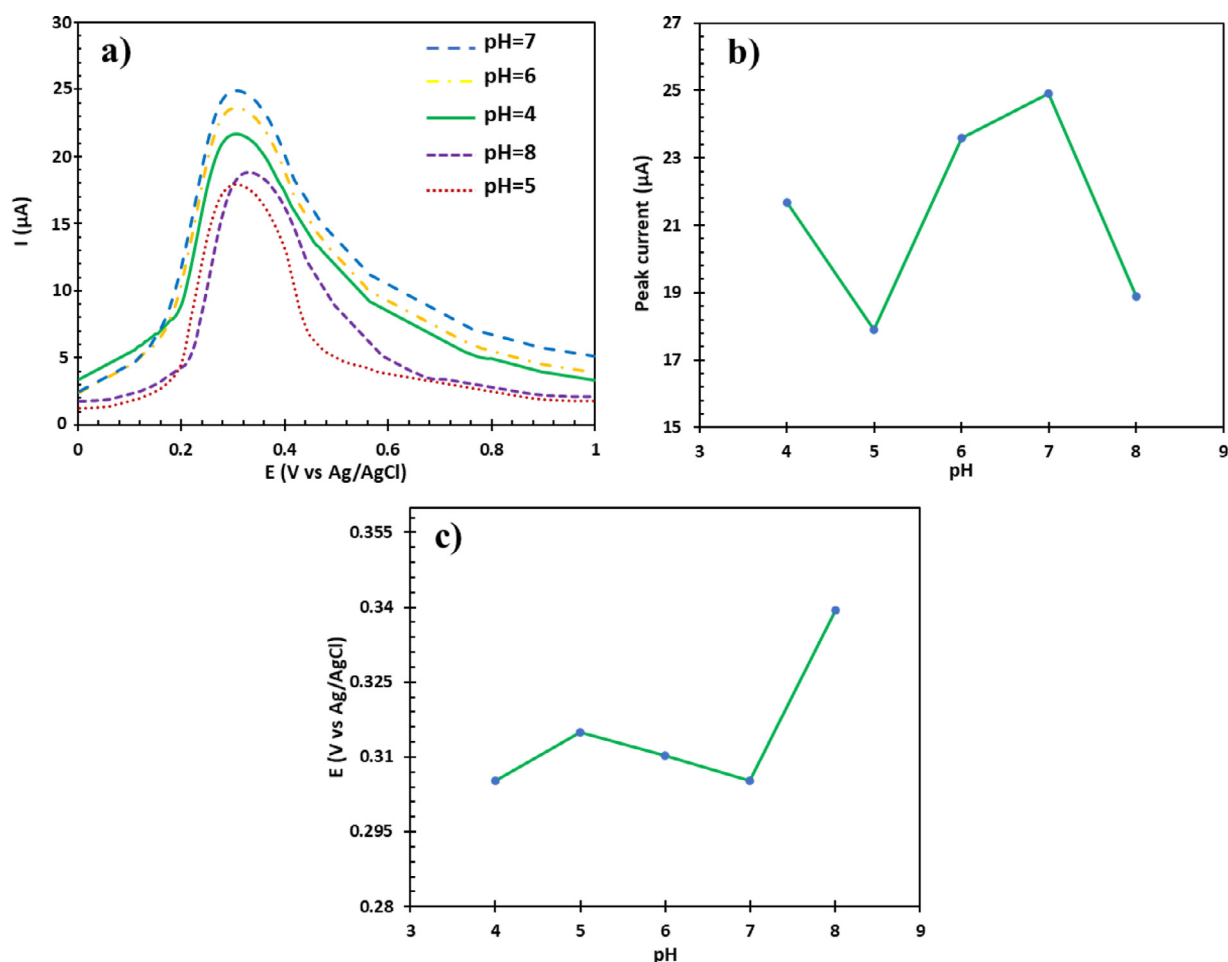


Fig. 13. (a) The effects of solution pH on the DPV peak current. (b) The relationship between DPV peak current and pH. (c) The relationship between DPV peak potential and pH.

0.16 μM , where σ and m were the blank standard deviation and the calibration plot slope, respectively. Also, the sensitivity of the sensor was calculated (slope of the calibration plot/active surface area (0.101 cm^2) of the modified electrode) as $1.55 \mu\text{A} \mu\text{M}^{-1} \text{cm}^{-2}$. Table 6 shows the comparison between the results of the present with other ferrocene-based research for dopamine determination; it is obvious that our fabricated electrode can compete in this field.

3.13. The interference study in the detection of dopamine

In continue, the interference study was performed using fabricated GC/BEFchTPB/(TFA+FEW) electrode in PBS 0.1 M at pH 7.0 spiked with 1 mM dopamine along with 1 mM ascorbic acid. The oxidation potential of ascorbic acid is very close to dopamine; since, the preparation of modified electrodes which is able to

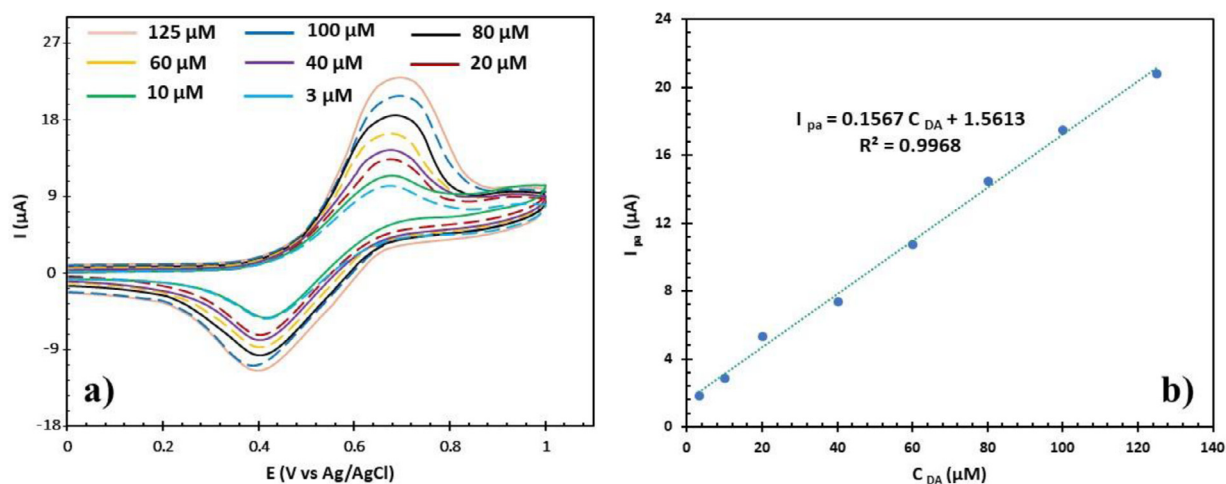


Fig. 14. (a) The relationship between peak current and dopamine concentration. (b) The calibration plot.

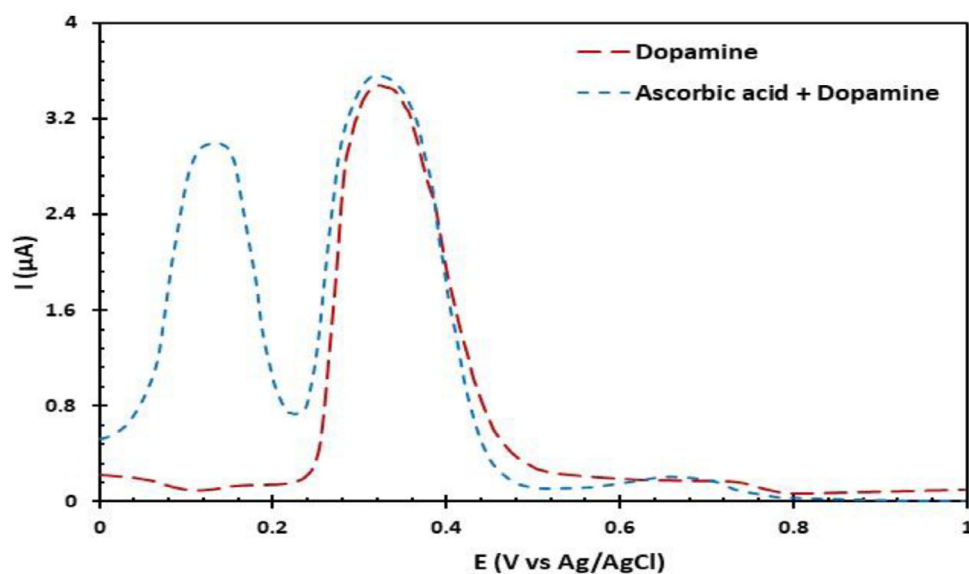
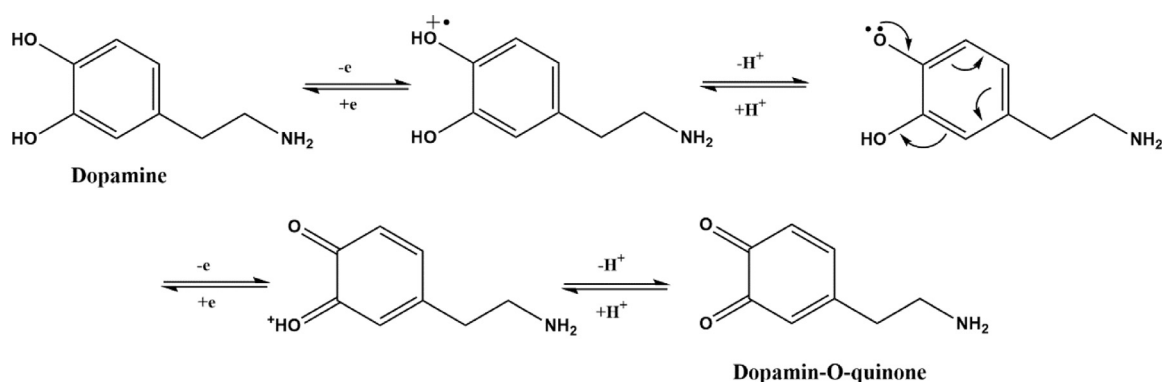


Fig. 15. DPV response GC/BEFCHTPB/(TFA+FEW) electrode for dopamine in the presence of ascorbic acid.

separate the oxidation peaks of dopamine and ascorbic acid is very attractive for scientists. Fig. 15 shows the oxidation potential 0.33 and 0.13 V for dopamine and ascorbic acid, respectively. The 0.20 V peak separations are large enough which allowing the determination of dopamine without interfering with the ascorbic acid.

3.14. Dopamine oxidation mechanism

The DA oxidation mechanism in pH = 7 is a two-electron and two-proton change process. As can be seen in Scheme 2, DA was oxidized and converted to dopamin-o-quinone.



Scheme 2. DA oxidation mechanism in pH = 7.

Table 6

The comparison of this work results with literatures.

Electrode	Linear response range (μM)	LOD (μM)	Ref.
FC/APTMS/GO	3–112	1.1	[56]
Nf/p(FcAni)-CNTsPE	1–150	0.21	[57]
GC/Fc@ β -CD	5–120	0.08	[58]
GC/Butacene/(TFA+FEW)	5–150	0.045	[52]
GC/BEFcHTPB/(TFA+FEW)	3–125	0.048	This work

4. Conclusion

In summary, we synthesized the bis-alkylferrocenyl silane grafted HTPB, via hydrosilylation reaction of bis-alkylferrocene based silane derivatives with HTPB in the presence of H_2PtCl_6 catalyst. Viscosity, iron content, and glass transition temperature of these new ferrocene grafted polymers were investigated. The predicted structures of the novel synthesized polymers were confirmed with FT-IR, ^1H -NMR, and MASS spectroscopy as well as CHN analysis. The electrochemical behavior of synthesized compounds was studied by cyclic voltammetry, and the relationship between the square root of scan rate and peak currents, showed that the redox process is diffusion-limited. On the other hand, presence of ferrocene caused the production of optical properties in the final polymer. We studied these properties using the UV-vis technique. Finally, the prepared polymer was drop-coated on the GCE surface, while cross-linking agents were FEW and TFA. The electrochemical behavior of the fabricated electrode was studied via EIS, CV, and DPV. The fabricated GC/BEFcHTPB/(TFA+FEW) electrode showed enhanced sensitivity in comparison to GCE for determination of dopamine in PBS. Additionally, based on interference study results, ascorbic acid did not have any interference with the determination of dopamine using GC/BEFcHTPB/(TFA+FEW) modified electrode. The most important limitations contain: can be affected by environmental changes and contamination, possibility of peeling the immobilized polymer from the electrode surface, and short shelf-life (maximum one month) of fabricated sensor.

Declaration of Competing Interest

The authors declare that they have no known competing financial interests or personal relationships that could have appeared to influence the work reported in this paper.

Acknowledgments

This project is supported by a research grant of the University of Tabriz (number SAD/796-970305).

References

- [1] R.A. Wise, M.A. Robble, Dopamine and addiction, *Annu. Rev. Psychol.* 71 (2020) 79–106, doi:10.1146/annurev-psych-010418-103337.
- [2] S.J. Park, J. Lee, S.E. Seo, K.H. Kim, C.S. Park, S.H. Lee, H.S. Ban, B.D. Lee, H.S. Song, J. Kim, C.S. Lee, High-performance conducting polymer nanotube-based liquid-ion gated field-effect transistor aptasensor for dopamine exocytosis, *Sci. Rep.* 10 (2020) 1–12, doi:10.1038/s41598-020-60715-x.
- [3] S. Palanisamy, S. Sakthianathan, S.M. Chen, B. Thirumalraj, T.H. Wu, B.S. Lou, X. Liu, Preparation of β -cyclodextrin entrapped graphite composite for sensitive detection of dopamine, *Carbohydr. Polym.* 135 (2016) 267–273, doi:10.1016/j.carbpol.2015.09.008.
- [4] S. Sakthianathan, S. Kubendhiran, S.M. Chen, K. Manibalan, M. Govindasamy, P. Tamizhdurai, S.T. Huang, Reduced graphene oxide non-covalent functionalized with zinc tetra phenyl porphyrin nanocomposite for electrochemical detection of dopamine in human serum and rat brain samples, *Electroanalysis* 28 (2016) 2126–2135, doi:10.1002/elan.201600085.
- [5] C. Karuppiyah, S. Sakthianathan, S.M. Chen, K. Manibalan, S.M. Chen, S.T. Huang, A non-covalent functionalization of copper tetraphenylporphyrin/chemically reduced graphene oxide nanocomposite for the selective determination of dopamine, *Appl. Organometal. Chem.* 30 (2016) 40–46, doi:10.1002/aoc.3397.
- [6] S. Palanisamy, K. Thangavelu, S.M. Chen, P. Gnanaprakasam, V. Velusamy, X.H. Liu, Preparation of chitosan grafted graphite composite for sensitive detection of dopamine in biological samples, *Carbohydr. Polym.* 151 (2016) 401–407, doi:10.1016/j.carbpol.2016.05.076.
- [7] S. Noori, P. Friedlich, I. Seri, Pharmacology review: developmentally regulated cardiovascular, renal, and neuroendocrine effects of dopamine, *Neo. Rev.* 4 (2003) e283–e288, doi:10.1542/neo.4-10-e283.
- [8] Y. Sun, Y. Lin, C. Ding, W. Sun, Y. Dai, X. Zhu, H. Liu, C. Luo, An ultrasensitive and ultrasensitive chemiluminescence aptasensor for dopamine detection based on aptamers modified magnetic mesoporous silica@ graphite oxide polymers, *Sens. Actuators B Chem.* 257 (2018) 312–323, doi:10.1016/j.snb.2017.10.171.
- [9] E.D. Zlotorzynska, Capillary electrophoresis in the determination of pollutants, *Electrophoresis* 18 (1997) 2453–2464, doi:10.1002/elps.1150181235.
- [10] M. Oh, E. Huh, M.S. Oh, J.S. Jeong, S.P. Hong, Development of a diagnostic method for Parkinson's disease by reverse-phase high-performance liquid chromatography coupled with integrated pulsed amperometric detection, *J. Pharm. Biomed.* 153 (2018) 110–116, doi:10.1016/j.jpba.2018.02.025.
- [11] K. Vuorensola, H. Sirén, U. Karjalainen, Determination of dopamine and methoxycatecholamines in patient urine by liquid chromatography with electrochemical detection and by capillary electrophoresis coupled with spectrophotometry and mass spectrometry, *J. Chromatogr. B* 788 (2003) 277–289, doi:10.1016/S1570-0232(02)01037-1.
- [12] X. Wei, Z. Zhang, Z. Wang, A simple dopamine detection method based on fluorescence analysis and dopamine polymerization, *Microchem. J.* 145 (2019) 55–58, doi:10.1016/j.microc.2018.10.004.
- [13] K. Jackowska, P. Kryszewski, New trends in the electrochemical sensing of dopamine, *Anal. Bioanal. Chem.* 405 (2013) 3753–3771, doi:10.1007/s00216-012-6578-2.
- [14] M. Sajid, N. Baig, K. Alhooshani, Chemically modified electrodes for electrochemical detection of dopamine: challenges and opportunities, *TrAC Trends Anal. Chem.* 118 (2019) 368–385, doi:10.1016/j.trac.2019.05.042.
- [15] N. Dükar, S. Tunç, K. Öztürk, S. Demirci, M. Dumangöz, M.S. Çelebi, F. Kuralay, Highly sensitive and selective dopamine sensing in biological fluids with one-pot prepared graphene/poly (o-phenylenediamine) modified electrodes, *Mater. Chem. Phys.* 228 (2019) 357–362, doi:10.1016/j.matchemphys.2019.02.043.
- [16] S. Sakthianathan, H.F. Lee, S.M. Chen, P. Tamizhdurai, Electrocatalytic oxidation of dopamine based on non-covalent functionalization of manganese tetraphenylporphyrin/reduced graphene oxide nanocomposite, *J. Colloid. Interface Sci.* 468 (2016) 120–127, doi:10.1016/j.jcis.2016.01.014.
- [17] Y. Wang, Y. Li, L. Tang, J. Lu, J. Li, Application of graphene-modified electrode for selective detection of dopamine, *Electrochem. Commun.* 11 (2009) 889–892, doi:10.1016/j.elecom.2009.02.013.
- [18] M. Baghayeri, M. Nodehi, H. Veisi, M.B. Tehrani, B. Maleki, M. Mehmoodost, The role of pramipexole functionalized MWCNTs to the fabrication of Pd nanoparticles modified GCE for electrochemical detection of dopamine, *DARU J. Pharm. Sci.* 27 (2019) 593–603, doi:10.1007/s40199-019-00287-y.
- [19] B. Demirkan, H. Ay, S. Karakuş, G. Uzun, A. Khan, F. Şen, Electrochemical detection of dopamine in the presence of uric acid using graphene oxide modified electrode as highly sensitive and selective sensors, *Graphene Funct. Strat.* (2019) 179–192, doi:10.1007/978-981-32-9057-0_7.
- [20] J. Cheng, X. Wang, T. Nie, L. Yin, S. Wang, Y. Zhao, H. Wu, H. Mei, A novel electrochemical sensing platform for detection of dopamine based on gold nanobipyramid/multi-walled carbon nanotube hybrids, *Anal. Bioanal. Chem.* 412 (2020) 1–9, doi:10.1007/s00216-020-02455-5.
- [21] I. Zablocka, M. Wysocka-Zolopa, K. Winkler, Electrochemical detection of dopamine at a gold electrode modified with a polypyrrole-mesoporous silica molecular sieves (MCM-48) film, *Int. J. Mol. Sci.* 20 (2019) 111–127, doi:10.3390/ijms20010111.
- [22] S. Palanisamy, V. Velusamy, S. Ramaraj, S.W. Chen, T.C. Yang, S. Balu, C.E. Banks, Facile synthesis of cellulose microfibers supported palladium nanospindles on graphene oxide for selective detection of dopamine in pharmaceutical and biological samples, *Mater. Sci. Eng. C* 98 (2019) 256–265, doi:10.1016/j.msec.2018.12.112.
- [23] S. Palanisamy, P. Yi-Fan, S.M. Chen, V. Velusamy, J.M. Hall, Facile preparation of a cellulose microfibers-exfoliated graphite composite: a robust sensor for determining dopamine in biological samples, *Cellulose* 24 (2017) 4291–4302, doi:10.1007/s10570-017-1425-4.
- [24] S. Palanisamy, S. Velmurugan, T.C. Yang, One-pot sonochemical synthesis of CuS nanoplates decorated partially reduced graphene oxide for biosensing of dopamine neurotransmitter, *Ultrason. Sonochem.* 64 (2020) 105043, doi:10.1016/j.ultrsonch.2020.105043.
- [25] M. Noroozifar, M. Khorasani-Motlagh, H.H. Nadiki, M.S. Hadavi, M.M. Foroughi, Modified fluorine-doped tin oxide electrode with inorganic ruthenium red dye-multiwalled carbon nanotubes for simultaneous determination of a dopamine, uric acid, and tryptophan, *Sens. Actuators B Chem.* 204 (2014) 333–341, doi:10.1016/j.snb.2014.07.060.
- [26] S. Sakthianathan, S.M. Chen, W.C. Liao, Multiwalled carbon nanotube supported Schiff base copper complex inorganic nanocomposite for enhanced electrochemical detection of dopamine, *Inorg. Chem. Front.* 4 (2017) 809–819, doi:10.1039/C7QJ00002B.
- [27] H. Miyaji, H. Komada, K. Goto, J. Fujimoto, N. Kiriya, J.H. Tucker, Selective recognition and electrochemical sensing of dopamine using a ferrocene-based heteroditopic receptor, *Tetrahedron Lett.* 59 (2018) 3853–3857, doi:10.1016/j.tetlet.2018.09.026.

- [28] M. Devendiran, K.K. Kumar, S.S. Narayanan, Fabrication of a novel Ferrocene/Thionin bimediator modified electrode for the electrochemical determination of dopamine and hydrogen peroxide, *J. Electroanal. Chem.* 802 (2017) 78–88, doi:[10.1016/j.jelechem.2017.08.016](https://doi.org/10.1016/j.jelechem.2017.08.016).
- [29] R. Rubio-Govea, D.P. Hickey, R. Garcia-Morales, M. Rodriguez-Delgado, M.A. Dominguez-Rovira, S.D. Minter, N. Ornelas-Soto, A. Garcia-Garcia, MoS₂ nanostructured materials for electrode modification in the development of a laccase based amperometric biosensor for non-invasive dopamine detection, *Microchem. J.* 155 (2020) 104792, doi:[10.1016/j.microc.2020.104792](https://doi.org/10.1016/j.microc.2020.104792).
- [30] F. Gao, X. Cai, X. Wang, C. Gao, S. Liu, F. Gao, Q. Wang, Highly sensitive and selective detection of dopamine in the presence of ascorbic acid at graphene oxide modified electrode, *Sens. Actuators B Chem.* 186 (2013) 380–387, doi:[10.1016/j.snb.2013.06.020](https://doi.org/10.1016/j.snb.2013.06.020).
- [31] W. Zhang, J. Zheng, J. Shi, Z. Lin, Q. Huang, H. Zhang, C. Wei, J. Chen, S. Hu, A. Hao, Nafion covered core-shell structured Fe₃O₄@graphene nanospheres modified electrode for highly selective detection of dopamine, *Anal. Chim. Acta.* 853 (2015) 285–290, doi:[10.1016/j.aca.2014.10.032](https://doi.org/10.1016/j.aca.2014.10.032).
- [32] S. Balu, S. Palanisamy, V. Velusamy, T.C. Yang, E.S.I. El-Shafey, Tin disulfide nanorod-graphene- β -cyclodextrin nanocomposites for sensing dopamine in rat brains and human blood serum, *Mater. Sci. Eng. C* 108 (2020) 110367, doi:[10.1016/j.msec.2019.110367](https://doi.org/10.1016/j.msec.2019.110367).
- [33] V. Jouikov, J. Simonet, Grafting of ω -Alkyl ferrocene radicals to carbon surfaces by means of electrocatalysis with subnanomolar transition-metal (Pd, Pt, or Au) layers, *Chem. Plus Chem.* 78 (2013) 70–76, doi:[10.1002/cplu.201200261](https://doi.org/10.1002/cplu.201200261).
- [34] D.W. Slocum, A.L. Edgecombe, J.S. Fowler, H.F. Gibbard, J. Phillips, Substituent effects on alkylferrocenes in molten salt mixtures, *J. Organomet. Chem.* 363 (1989) 151–155, doi:[10.1016/0022-328X\(89\)88048-9](https://doi.org/10.1016/0022-328X(89)88048-9).
- [35] A.D. Ryabov, Transition metal chemistry of glucose oxidase, horseradish peroxidase, and related enzymes, *Adv. Inorg. Chem.* 55 (2004) 201–269, doi:[10.1016/S0898-8838\(03\)55004-8](https://doi.org/10.1016/S0898-8838(03)55004-8).
- [36] V.A. Ol'shevskaya, M.D. Kotova, E.G. Kononova, A.S. Peregodov, V.N. Kalinin, Ferrocenyl substituted oxo-derivatives of carboranes: synthesis and some chemical transformations, *Polyhedron* 85 (2015) 27–33, doi:[10.1016/j.poly.2014.08.015](https://doi.org/10.1016/j.poly.2014.08.015).
- [37] M.A. Bazhenova, S.S. Bogush, A.G. Herbst, T.V. Demeshchik, Y.G. Komarovskaya, V.S. Kurova, M.D. Reshetova, A.D. Ryabov, E.S. Ryabova, Y.N. Frrsova, Synthesis and electrochemical properties of mono- and (\pm)-1, 2-dialkylferrocenes and alkylferrocenium hexafluorophosphates in aqueous and micellar media, *Russ. Chem. Bull.* 45 (1996) 2445–2451, doi:[10.1007/BF01435401](https://doi.org/10.1007/BF01435401).
- [38] K.L. Rinehart Jr, A.F. Ellis, C.J. Michejda, P.A. Kittle, Acyl-from alkyl-ferrocenes by manganese dioxide oxidation. Ferrocenobenzoquinone, *J. Am. Chem. Soc.* 82 (1960) 4112–4113, doi:[10.1021/ja01500a075](https://doi.org/10.1021/ja01500a075).
- [39] S. Bhattacharyya, Titanium (IV) Chloride–Triethylsilane: an efficient, mild system for the reduction of acylferrocenes to alkylferrocenes, *J. Org. Chem.* 63 (1998) 7101–7102, doi:[10.1021/jo980685](https://doi.org/10.1021/jo980685).
- [40] F. Szillat, B.V. Schmidt, A. Hubert, C. Barner-Kowollik, H. Ritter, Redox-Switchable supramolecular graft polymer formation via ferrocene-cyclodextrin assembly, *Macromol. Rapid. Commun.* 35 (2014) 1293–1300, doi:[10.1002/marc.201400122](https://doi.org/10.1002/marc.201400122).
- [41] R. Teimuri-Mofrad, H. Abbasi, R. Hadi, Graphene oxide-grafted ferrocene moiety via ring opening polymerization (ROP) as a supercapacitor electrode material, *Polymer* 167 (2019) 138–145, doi:[10.1016/j.polymer.2019.01.084](https://doi.org/10.1016/j.polymer.2019.01.084).
- [42] A. Jiménez, M.P.G. Armada, J. Losada, C. Villena, B. Alonso, C.M. Casado, Amperometric biosensors for NADH based on hyperbranched dendritic ferrocene polymers and Pt nanoparticles, *Sens. Actuators B* 190 (2014) 111–119, doi:[10.1016/j.snb.2013.08.072](https://doi.org/10.1016/j.snb.2013.08.072).
- [43] A.R. Kazemizadeh, N. Shajari, R. Shapouri, N. Adibpour, R. Teimuri-Mofrad, Synthesis and anti-brucella activity of some new 1, 3, 4-oxadiazole derivatives containing a ferrocene unit, *J. Iran. Chem. Soc.* 13 (2016) 1349–1355, doi:[10.1007/s13738-016-0849-3](https://doi.org/10.1007/s13738-016-0849-3).
- [44] T. Lanez, M. Henni, Antioxidant activity and superoxide anion radical interaction with 2-(ferrocenylmethylamino) benzonitrile and 3-(ferrocenylmethylamino) benzonitrile, *J. Iran. Chem. Soc.* 13 (2016) 1741–1748, doi:[10.1007/s13738-016-0891-1](https://doi.org/10.1007/s13738-016-0891-1).
- [45] D. Saravanakumar, N. Sengottuvelan, V. Narayanan, M. Kandaswamy, T.L. Varghese, Burning-rate enhancement of a high-energy rocket composite solid propellant based on ferrocene-grafted hydroxyl-terminated polybutadiene binder, *J. Appl. Polym. Sci.* 119 (2011) 2517–2524, doi:[10.1002/app.32859](https://doi.org/10.1002/app.32859).
- [46] B.N. Rao, K. Malkappa, N. Kumar, T. Jana, Ferrocene grafted hydroxyl terminated polybutadiene: a binder for propellant with improved burn rate, *Polymer* 163 (2019) 162–170, doi:[10.1016/j.polymer.2019.01.008](https://doi.org/10.1016/j.polymer.2019.01.008).
- [47] R. Teimuri-Mofrad, K.D. Safa, S. Abedinpour, K. Rahimpour, Synthesis of 5-(dimethylsilyl) pentylalkylferrocene-grafted HTPB (alkylFc-HTPB) via platinum-catalyzed hydrosilylation, *J. Iran. Chem. Soc.* 14 (2017) 2177–2185, doi:[10.1007/s13738-017-1154-5](https://doi.org/10.1007/s13738-017-1154-5).
- [48] K. Rahimpour, R. Teimuri-Mofrad, H. Abbasi, M. Parchehbaf, S. Abedinpour, S. Soleimani, Synthesis, characterization and properties investigation of [4-(Dimethylsilyl) butyl] alkylferrocene Grafted HTPB as novel ferrocene based burning rate accelerator catalysts for composite gas generators, *Poly-Plast. Technol. Mater.* (2019) 1–10, doi:[10.1080/25740881.2019.1625383](https://doi.org/10.1080/25740881.2019.1625383).
- [49] a) R. Teimuri-Mofrad, R. Hadi, H. Abbasi, R.F.B. Baj, Synthesis, characterization and electrochemical study of carbon nanotube/chitosan-ferrocene nanocomposite electrode as supercapacitor material, *J. Electron. Mater.* 48 (2019) 4573–4581, doi:[10.1007/s11664-019-07226-2](https://doi.org/10.1007/s11664-019-07226-2); b) R. Teimuri-Mofrad, R. Hadi, H. Abbasi, Synthesis and characterization of ferrocene-functionalized reduced graphene oxide nanocomposite as a supercapacitor electrode material, *J. Organomet. Chem.* 880 (2019) 355–362, doi:[10.1016/j.jorganchem.2018.11.033](https://doi.org/10.1016/j.jorganchem.2018.11.033).
- [50] R. Teimuri-Mofrad, K.D. Safa, K. Rahimpour, Synthesis, characterization and electrochemical properties of novel trinuclear ferrocenyl based organosilane compounds, *J. Organomet. Chem.* 758 (2014) 36–44, doi:[10.1016/j.jorganchem.2014.02.001](https://doi.org/10.1016/j.jorganchem.2014.02.001).
- [51] R. Teimuri-Mofrad, S. Esmati, S. Tahmasebi, M. Gholamhosseini-Nazari, Bisferrocene-containing ionic liquid supported on silica coated Fe₃O₄: A novel nanomagnetic catalyst for the synthesis of dihydropyran [2, 3-c] coumarin derivatives, *J. Organomet. Chem.* 870 (2018) 38–50, doi:[10.1016/j.jorganchem.2018.06.007](https://doi.org/10.1016/j.jorganchem.2018.06.007).
- [52] K. Rahimpour, R. Teimuri-Mofrad, Electrocatalytic oxidation of dopamine on the surface of ferrocene grafted hydroxyl terminated polybutadiene modified electrode, *Polymer* (2020) 122310, doi:[10.1016/j.polymer.2020.122310](https://doi.org/10.1016/j.polymer.2020.122310).
- [53] B. Fang, W. Zhang, X. Kan, H. Tao, X. Deng, M. Li, Fabrication and application of a novel modified electrode based on β -cyclodextrin/ferrocenecarboxylic acid inclusion complex, *Sens. Actuators B Chem.* 117 (2006) 230–235, doi:[10.1016/j.snb.2005.11.027](https://doi.org/10.1016/j.snb.2005.11.027).
- [54] A.S. Kumar, P. Swetha, K.C. Pillai, Enzyme-less and selective electrochemical sensing of catechol and dopamine using ferrocene bound Nafion membrane modified electrode, *Anal. Methods* 2 (2010) 1962–1968, doi:[10.1039/C0AY00430H](https://doi.org/10.1039/C0AY00430H).
- [55] C.R. Raj, T. Ohsaka, Electroanalysis of ascorbate and dopamine at a gold electrode modified with a positively charged self-assembled monolayer, *J. Electroanal. Chem.* 496 (2001) 44–49, doi:[10.1016/S0022-0728\(00\)00335-1](https://doi.org/10.1016/S0022-0728(00)00335-1).
- [56] M. Elanchezian, D. Manoj, D. Saravanakumar, K. Thenmozhi, S. Senthilkumar, Amperometric sensing of catechol using a glassy carbon electrode modified with ferrocene covalently immobilized on graphene oxide, *Microchim. Acta* 184 (2017) 2925–2932, doi:[10.1007/s00604-017-2312-2](https://doi.org/10.1007/s00604-017-2312-2).
- [57] W. Sroysee, S. Chairam, M. Amatatongchai, P. Jarujamrus, S. Tamuang, S. Pim-mongkol, L. Chaicharoenwimolkul, E. Somsook, Poly (m-ferrocenylaniline) modified carbon nanotubes-paste electrode encapsulated in nafion film for selective and sensitive determination of dopamine and uric acid in the presence of ascorbic acid, *J. Saudi Chem. Soc.* 22 (2018) 173–182, doi:[10.1016/j.jscs.2016.02.003](https://doi.org/10.1016/j.jscs.2016.02.003).
- [58] H. Zhang, P. Dai, L. Huang, Y. Huang, Q. Huang, W. Zhang, C. Wei, S. Hu, A nitrogen-doped carbon dot/ferrocene@ β -cyclodextrin composite as an enhanced material for sensitive and selective determination of uric acid, *Anal. Methods* 6 (2014) 2687–2691, doi:[10.1039/C4AY00140K](https://doi.org/10.1039/C4AY00140K).